

A NEW SAUROPOD DINOSAUR FROM THE LATE JURASSIC OF CHINA AND THE DIVERSITY, DISTRIBUTION, AND RELATIONSHIPS OF MAMENCHISAURIDS

LIDA XING,¹ TETSUTO MIYASHITA,^{*2} JIANPING ZHANG,¹ DAQING LI,³ YONG YE,⁴ TORU SEKIYA,⁵
FENGPING WANG,⁶ and PHILIP J. CURRIE²

¹School of the Earth Sciences and Resources, China University of Geosciences, Beijing 100083, China, xinglida@gmail.com;
zhjping@cugb.edu.cn;

²Department of Biological Sciences, University of Alberta, Edmonton, Alberta, Canada T6G 2E9, tetsuto@ualberta.ca;
philip.currie@ualberta.ca;

³Geological Museum of Gansu Province, Lanzhou 730040, China, daqingligs@gmail.com;

⁴Zigong Dinosaur Museum, 238, Dashanpu, Zigong 643013, Sichuan, China, yeyozdm@126.com;

⁵Fukui Prefectural Dinosaur Museum, Katsuyama, Fukui, Japan 911-8601, t.sekiya.jiu@gmail.com;

⁶Qijiang County Bureau of Land and Resources, Chongqing 401420, China, 455039424@qq.com

ABSTRACT—*Qijianglong guokr*, gen. et sp. nov., represents a mamenchisaurid eusauropod from the Late Jurassic of southern China. The holotype consists of an incomplete skull, partly articulated axial skeleton, and fragmentary appendicular skeleton. A well-preserved braincase and skull roof provide rare insights into the poorly known neurocranial anatomy of mamenchisaurids and reveal a unique combination of characters such as an accessory tuber at the base of planar basiptyergoid process and parietal excluding frontal from the anterior margin of the supratemporal fenestra. The cervical vertebrae have a distinct finger-like process extending from the postzygapophyseal process beside a zygapophyseal contact. *Qijianglong* is the first mamenchisaurid from the Late Jurassic of China that is definitively distinct from *Mamenchisaurus*, indicating greater morphological and taxonomic diversity of the poorly represented Late Jurassic mamenchisaurids. The occurrence of *Qijianglong* is consistent with a scenario in which mamenchisaurids formed an endemic sauropod fauna in the Late Jurassic of Asia. Phylogenetically, *Qijianglong* represents a relatively plesiomorphic mamenchisaurid lineage. The mamenchisaurids form an ancient clade of basal eusauropod dinosaurs that likely appeared in the Early Jurassic. A cladistic analysis highlights the interrelationships of mamenchisaurids and suggests guidelines for mamenchisaurid taxonomic revision. It may be desirable to restrict generic names to the type species in order to avoid confusion.

<http://zoobank.org/urn:lsid:zoobank.org:pub:F93276CF-71FE-472E-9114-68294547C2A9>

SUPPLEMENTAL DATA—Supplemental materials are available for this article for free at www.tandfonline.com/UJVP

INTRODUCTION

The sauropod fauna from the Late Jurassic of Asia has previously been considered distinct from the contemporaneous sauropod faunas from other landmasses in two respects: (1) the dominance of mamenchisaurids, which likely form a clade of basal eusauropods; and (2) the absence of definitive diplodocoids and titanosauriforms (Upchurch et al., 2004; Mannion et al., 2011; Whitlock et al., 2011). Mamenchisaurids replaced a diverse assemblage of basal eusauropods and possible macronarian neosauropods in the Late Jurassic of Asia (Xing et al., 2013). The dominance of titanosauriform neosauropods followed in the Early Cretaceous (Whitlock et al., 2011). The faunal turnovers amongst sauropods of different phylogenetic grades seemingly correlate with the geographic isolation and reconnection of Asia during the Late Jurassic (Russell, 1993; Upchurch and Mannion, 2009; Mannion et al., 2011; Whitlock et al., 2011). This correlation suggests that the Late Jurassic sauropods from Asia represent an endemic fauna. All mamenchisaurids from this critical time interval have been assigned to the single genus *Mamenchisaurus*. Thus, the Late Jurassic times appears to have been a bottleneck in Asian sauropod diversity, with low morphological and

systematic diversities. Alternatively, the diversity may be underestimated. It is possible that the genus *Mamenchisaurus* merely serves as a wastebasket taxon for large basal eusauropods from the Late Jurassic of Asia. However, it has been difficult to evaluate either of the hypotheses because of the lack of comparative studies, and because of the lack of cranial materials in many of the species.

This biostratigraphic and biogeographic scheme for Asian sauropods faces a modest challenge from revised chronological correlations of the Jurassic localities in the Sichuan Basin. The upper Shaximiao succession (Shangshaximiao) was recently resolved as upper Middle Jurassic in age (Bathonian–Callovian; G. Li et al., 2010; K. Li et al., 2010a; Wang et al., 2010). This revised chronology reassigns the majority of sauropod taxa that occur in the upper successions of the Jurassic Sichuan Basin from the lower Upper Jurassic to the upper Middle Jurassic (Table 1). This revision leaves only two valid sauropod taxa as definitively Late Jurassic taxa from China: *Mamenchisaurus anyuensis* from the Suining Formation (He et al., 1996) and *M. sino-canadorum* from the upper Shishugou Formation (Russell and Zheng, 1993). The postcranial skeletons from the Xiangtang Formation are referred to *M. constructus* (Young, 1958), but this assignment is inadequate in the light of multiple species of *Mamenchisaurus* and the lack of description of diagnostic

*Corresponding author.

TABLE 1. Chronological distribution of sauropodomorphs from the Early Jurassic to Early Cretaceous of Asia.

Early Jurassic	Middle Jurassic
Sauropodomorpha	Sauropodomorpha
<i>Chuxiongosaurus lufengensis</i> ILU	<i>Yunnanosaurus youngi</i> ZG
<i>Jingshanosaurus xinwaensis</i> ILU	Eusauropoda
<i>Lufengosaurus huenei</i> ILU, ZZ	<i>Chuanjiesaurus anaensis</i> CH
<i>Xixiposaurus suni</i> ILU	<i>Datousaurus bashanensis</i> ISX
<i>Yimenosaurus youngi</i> FJ	<i>Hudiesaurus sinojapanorum</i> * QG
<i>Yunnanosaurus huangi</i> ILU	<i>Nebulasaurus taito</i> ZG
<i>Yunnanosaurus robustus</i> FJ/ZG	<i>Shunosaurus lii</i> ISX
Sauropoda	Mamenchisauridae
<i>Chinshakiangosaurus chunghoensis</i> FJ	<i>Eomamenchisaurus yuanmouensis</i> ZG
<i>Gongxianosaurus shibeiensis</i> ZL	<i>Mamenchisaurus constructus</i> uSX
Eusauropoda	<i>Mamenchisaurus fuxiensis</i> ISX
Mamenchisauridae	<i>Mamenchisaurus hochuanensis</i> uSX
<i>Tonganosaurus hei</i> YM	<i>Mamenchisaurus jingyanensis</i> uSX
	<i>Mamenchisaurus youngi</i> uSX
	<i>Omeisaurus jiaoi</i> ISX
	<i>Omeisaurus junghsiensis</i> ISX
	<i>Omeisaurus maoianus</i> uSX
	<i>Omeisaurus tianfuensis</i> ISX
	<i>Xinjiangtitan shanshanensis</i> QG
	? <i>Yuanmousaurus jingyiensis</i> § ZG
	Neosauropoda
	<i>Ferganasaurus verzilini</i> BB
	Macronaria
	<i>Abrosaurus dongpoi</i> ISX
	<i>Bellusaurus sui</i> WC
	<i>Daanosaurus zhangii</i> uSX
Late Jurassic	Early Cretaceous
Sauropodomorpha	Sauropodomorpha
Eusauropoda	Neosauropoda
Mamenchisauridae	Macronaria
<i>Mamenchisaurus anyuensis</i> uSU	Titanosauriformes
<i>Mamenchisaurus sinocanadorum</i> uSS	<i>Chiyusaurus lacustris</i> KZ
? <i>Mamenchisaurus constructus</i> ‡ XT	<i>Daxiatitan binglingi</i> NP
? <i>Mamenchisaurus</i> sp. PK	<i>Dongbeititan dongi</i> YX
<i>Qijianglong guokr</i> , gen. et sp. nov. SU	<i>Erketu ellisoni</i> BS
	<i>Euhelopus zdankyi</i> MY
	<i>Fukuittitan nipponensis</i> KD
	<i>Fusuisaurus zhaoui</i> NP
	<i>Gobititan shenzhouensis</i> DG
	<i>Huanghetitan liujiaxiaensis</i> HK
	<i>Jiangshanosaurus lixianensis</i> JH
	<i>Jiutaisaurus xidiensis</i> QT
	<i>Liubangosaurus hei</i> NP
	<i>Mongolosaurus haplodon</i> OG
	<i>Phuwiangosaurus sirindhornae</i> SK
	<i>Pukyongosaurus millenniumi</i> HD
	<i>Qiaowanlong kangxii</i> XM
	<i>Tangvayosaurus hoffeti</i>
	<i>Yunmenglong ruyangensis</i> HL

This table is a revision of that in Xing et al. (2013). The upper Shaximiao Formation is now regarded as the upper Middle Jurassic (Bathonian–Callovia). *Qijianglong* (this paper), *Xijiangtitan* (Wu et al., 2013), and *Yunmenlong* (Lü et al., 2013) are added. Each taxon is denoted with two upper case letters that stand for the stratigraphic unit from which it derives. Where a single formation contains demonstrably distinct faunas between upper and lower levels, a lower case letter indicates whether the taxon occurs in the upper (u) or lower (l) levels. This list does not include taxa that are considered not diagnosable in the current literature, such as *Tienschanosaurus* (Upchurch et al., 2004) and *Yuanmousaurus* (Xing et al., 2013). **Abbreviations:** **BB**, Balabansai Formation; **BS**, Baynshiree Svita; **CH**, Chuanjie Formation; **DG**, Digou Formation; **FJ**, Fengjiahe Formation; **GS**, Grès Supérieur Formation; **HD**, Hasandong Formation; **HK**, Hekou Group; **HL**, Haoling Formation; **JH**, Jinhua Formation; **KD**, Kitadani Formation; **KZ**, Kalazha Formation; **LU**, Lufeng Formation; **MY**, Mengyin Formation; **NP**, Napai Formation; **OG**, On Gong Formation; **PK**, Phu Kradung Formation; **QG**, Qigu Formation; **QT**, Quantou Formation; **SK**, Sao Khua Formation; **SU**, Suining Formation; **SS**, Shishugou Formation; **SX**, Shaximiao Formation; **WC**, Wucaiwan Formation; **XM**, Xinminpu Group; **XT**, Xiangtang Formation; **YM**, Yimen Formation; **YX**, Yixian Formation; **ZG**, Zhanghe Formation; **ZL**, Ziliujing Formation; **ZZ**, Zhenzhuchong Formation.

*Chronological age is uncertain. The type and only specimen of *Hudiesaurus* likely comes from the upper Middle Jurassic Qigu Formation (Wings et al., 2011, 2012).

§Taxonomic status is uncertain. This taxon may represent an indeterminate mamenchisaurid (Xing et al., 2013).

‡Postcranial skeletons are referred to *M. constructus* (Young, 1958). Pending description of proper diagnostic characters, it remains uncertain whether or not these specimens pertain to the taxon.

§Taxonomic status and chronological age are uncertain; from the Late Jurassic/Early Cretaceous of Thailand (Phu Kradung Formation; Suteethorn et al., 2013).

characters. *Hudiesaurus sinojapanorum* was initially reported from the Upper Jurassic Kalazha Formation of Xinjiang, but the original material was likely collected from the upper Middle Jurassic Qigu Formation (Wings et al., 2011, 2012). Despite its problematic taxonomy and despite the coarsely sampled Late Jurassic record, *Mamenchisaurus* remains as the only sauropod genus in the Late Jurassic of China.

The majority of the Middle–Late Jurassic sauropods from China occur in the Sichuan Basin, which makes this a primary locality for a revision of mamenchisaurids. In contrast to the rich vertebrate fauna from the Middle Jurassic Shaximiao Formation in the basin, however, dinosaur fossils are rare in the overlying Upper Jurassic Suining and Penglaizhen formations (Zhang and Li, 2003). The sole valid sauropod taxon from these formations is *M. anyuensis*. This species is represented by teeth and postcranial skeletons of more than 10 individuals from the Suining Formation (He et al., 1996) and by another 70% complete postcranial skeleton from the uppermost Suining Formation just below the contact with the overlying Penglaizhen Formation (Ouyang and Ye, 2002). Additional sauropod materials were collected from the Longjiaya fossil site in Anyue County (Kan et al., 2005), but the materials have not been described. The youngest record of *Mamenchisaurus* from China is fragmentary postcranial material tentatively assigned to *M. anyuensis* from the Penglaizhen Formation (He et al., 1996).

As a lead to the elusive vertebrate fossils from the Suining Formation, a local farmer (Cai Changming) discovered sauropod vertebrae in his backyard in Heba Village, Beidu Township, in the early 1990s. In 2006, construction workers working 500 m from the original locality spotted a 0.7 m long neopterygian fish (*Lepidotes*). These discoveries prompted Qijiang District to commission a survey of the area by the Fossil Research and Development Center of the Third Geology and Mineral Resources Exploration Academy of Gansu Province. A new mamenchisaurid sauropod was discovered during this field work. This paper presents a description of the sauropod, *Qijianglong guokr*, gen. et sp. nov., based on morphological features unique among mamenchisaurids, such as extensive pneumatization of the cervical vertebrae. *Qijianglong* improves the resolution of mamenchisaurid interrelationships, hints at an imminent taxonomic revision for multiple mamenchisaurid taxa, and strengthens the endemism scenario for the Late Jurassic Asian sauropod fauna.

Institutional Abbreviations—PMU, Paleontological Museum of Uppsala University, Uppsala, Sweden; QJGPM, Qijiang Petrified Wood and Dinosaur Footprint National Geological Park Museum, Chongqing, China; ZDM, Zigong Dinosaur Museum, Zigong, Sichuan, China.

SYSTEMATIC PALEONTOLOGY

SAURISCHIA Seeley, 1887
 SAUROPODOMORPHA Huene, 1932
 SAUROPODA Marsh, 1878
 EUSAUROPODA Upchurch, 1995
 MAMENCHISAURIDAE Young and Chao, 1972
QIJIANGLONG, gen. nov.

Type and Only Known Species—*Qijianglong guokr*, sp. nov.

Etymology—Qijiang, after Qijiang District where the type specimen was collected and is accessioned; ‘long,’ dragon in Chinese.

Diagnosis—As for the type and only known species.

QIJIANGLONG GUOKR, sp. nov.
 (Figs. 2–14)

Holotype—QJGPM 1001. Skull consisting of the skull roof, braincase, right pterygoid, fragments of right antorbital elements (lacrimal, maxilla, palatine, ectopterygoid), right postorbital, and

right quadrate; a complete cervical series; thoracic dorsal series; distal caudal series; numerous fragments of neural arches; numerous rib fragments; numerous hemal arch fragments; left pubis; and a pedal phalanx.

Horizon—Suining Formation (Upper Jurassic). Seven formations of terrestrial deposits represent the Jurassic of the Sichuan Basin (in ascending order): Zhenzhuchong, Ziliujing, Xintian-gou, Xiashaximiao (lower Shaximiao), Shangshaximiao (upper Shaximiao), Suining, and Penglaizhen formations (Peng et al., 2005). The last two formations are calibrated to the Upper Jurassic part of the succession. The Suining Formation overlies the lower Shangshaximiao Formation, with a single lithology predominated by red and reddish-brown calcareous mudstone, mixed with some off-white and gray-green quartz sandstone. Based on the lithology and the characteristics of associated ostracods, the stratigraphic age of the Suining Formation is definitively Upper Jurassic (Gu and Li, 1997; Peng et al., 2005; G. Li et al., 2010; Wang et al., 2010; Xie et al., 2010).

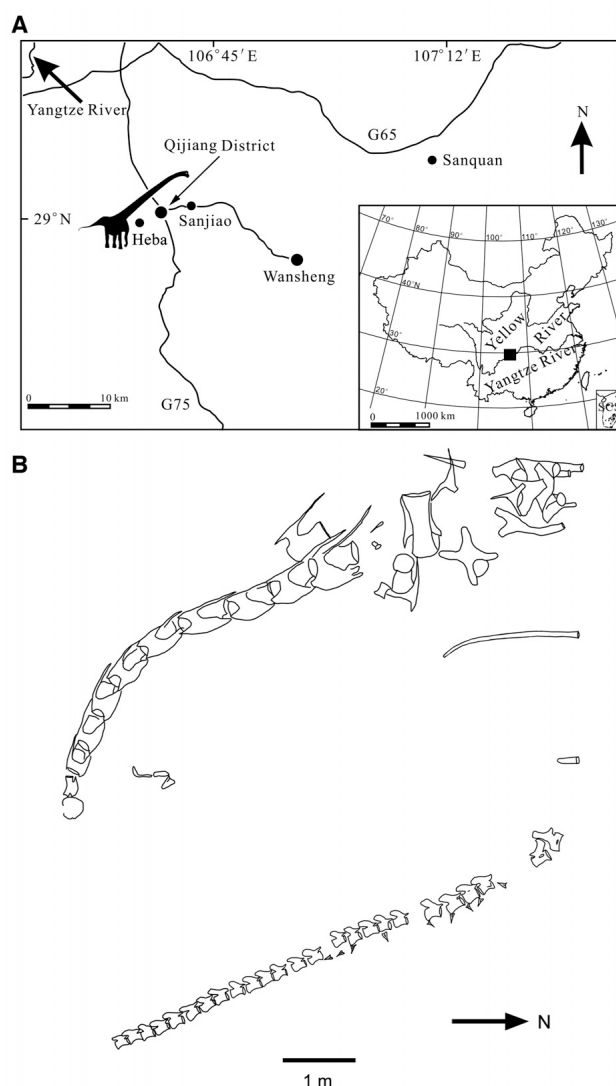


FIGURE 1. Geographic and taphonomic information on the holotype of *Qijianglong guokr* (QJGPM 1001). **A**, location of the locality for QJGPM 1001 (indicated by a silhouette of a sauropod) and Qijiang District in China (inset map); **B**, site map for QJGPM 1001. The skull elements were found in the block indicated by a circle at the end of the cervical series.

Locality—Beidu site (29°0'25"N, 106°34'55"E), Qijiang Petrified Wood and Dinosaur Footprint National Geological Park, Qijiang District, Chongqing Municipality, China (Fig. 1A). The outcrops within the park consist of the Shangshaximiao, Suining, and Penglaizhen formations and the mid-Cretaceous Jiaguan Formation. The fossil assemblage from the Upper Jurassic strata in the park includes coniferopsid petrified wood, theropod teeth (Wang Feng-ping, pers. comm., 2011), and the sauropod remains described in this paper.

Etymology—*guokr* (gu-OH-ke-r), named in honor of Guokr (science social network; 'nutshell' in Chinese) for their support of paleontology in Qijiang.

Diagnosis—A non-neosauropod basal eusauropod with the following unique combination of characters and autapomorphies: (1) semi-equal anteroposterior lengths of frontal and parietal (also in *Omeisaurus* and *Shunosaurus*); (2) parietal forming the entire anterior margin of supratemporal fenestra (also in *Atlasaurus* and *Omeisaurus*); (3) absence of frontoparietal fenestra and presence of postparietal foramen (also in *Spinophorosaurus*); (4) plate-like basiptyergoid process oriented anteroventrally with an accessory tuber paralleling basal tuber (autapomorphy); (5) a finger-like process lateral to postzygapophyses in cervical vertebrae (autapomorphy); (6) pneumatopores in spinodiapophyseal fossa in posterior cervical vertebrae (autapomorphy); (7) anterior outline of spinous process of mid-caudal vertebra indented posteriorly for more than half a length of centrum (also in *Mamenchisaurus*); and (8) pubis anteriorly concave such that the distal end points more anteriorly than ventrally (autapomorphy). Numbers refer to each diagnostic character indicated by an arrow in relevant figures (Figs. 2, 5, 11, 12, 14, 15).

DESCRIPTION

Skull

The incomplete skull consists of six fractured portions, each collected as a single block from the quarry (postorbital, pterygoid, quadrate, skull roof–facial unit, occipital plane, and basicranium). The largest portion (Fig. 2) includes the right maxilla, right lacrimal, right palatine, right ectopterygoid, prefrontals, frontals, and parietals. Among these elements, the only visible suture is between the frontals and parietals. The maxilla, palatine, and ectopterygoid are only fragmentarily preserved and cannot be compared with other sauropod skulls. These facial and palatal elements and the lacrimal are set in a vertical plane perpendicular to the skull roof, which does not accurately reflect their respective positions in life. A crack at the anterior end of the skull roof through the prefrontal indicates that the preorbital bar was at an angle about 5° shallower than perpendicular to the skull roof.

Frontals and Parietals—The frontals and parietals form a flat skull roof that is as long anteroposteriorly as it is wide transversely (Fig. 2). The anteroposterior length of the frontal is only 10% longer than the maximum anteroposterior length of the parietal. The semi-equal proportions of length of the frontals and parietals also exist in *Omeisaurus tianfuensis* and *Shunosaurus* (He et al., 1988; Chatterjee and Zheng, 2002), whereas the frontals are longer anteroposteriorly than the parietals in other basal sauropods such as *Jobaria*, *Mamenchisaurus youngi*, and *Spinophorosaurus* as well as in many derived taxa (Serenio et al., 1999; Ouyang and Ye, 2002; Knoll et al., 2012). In dorsal view, the orbital margin is gently concave laterally. The frontals meet the parietals along the suture that forms a shallow, posteriorly pointed 'V' of approximately 150°. The parietal extends anterolaterally to form the entire anterior margin of the supratemporal fenestra as in *Atlasaurus* and *O. tianfuensis* (He et al., 1988; Monbaron et al., 1999). The postorbital participates in this margin in *Jobaria*, *M. youngi*, and *Spinophorosaurus*, but even in

these sauropods the frontal is excluded from the supratemporal fenestra by both the parietal and postorbital (Serenio et al., 1999; Ouyang and Ye, 2002; Remes et al., 2009; Knoll et al., 2012). In *Shunosaurus* and *Turiasaurus*, the frontal participates in the margin of the fenestra (Chatterjee and Zheng, 2002; Royo-Torres and Upchurch, 2012). The supratemporal fenestra is transversely wider than anteroposteriorly long as in most sauropods, but the proportions are reversed in *M. youngi* and *Turiasaurus* (Ouyang and Ye, 2002; Royo-Torres and Upchurch, 2012). As is the case for most sauropods, the supratemporal fenestra is not enclosed within a fossa in *Qijianglong*.

Whereas a frontoparietal fenestra is absent, the postparietal foramen demarcates the posterior end of the parietal at the midline. The posterior wing of the parietal is oriented posterolaterally. In ventral view, both the frontals and parietals preserve impressions of various parts of the brain. The dural depression is longer anteroposteriorly than wide transversely and deeper posteriorly toward the postparietal foramen. The depression is not divided bilaterally. In comparison with the previously described cranial endocasts of sauropods, this depression likely housed the dural peak and a longitudinal venous sinus rather than the cerebral hemispheres. Anteriorly, the ventral surface of the frontal has the impressions of the cerebral hemispheres and olfactory tract. At the anterior end of the tract is a pair of small depressions for the olfactory bulbs. These depressions are narrower transversely but deeper than the olfactory tract and clearly separated at the midline. The profile of an endocast reconstructed from these impressions generally agrees with the three-dimensionally reconstructed cranial endocasts of *Ampelosaurus*, *Apatosaurus*, *Brachiosaurus*, *Camarasaurus*, *Dicraeosaurus*, *Diplodocus*, *Nigersaurus*, *Shunosaurus*, *Spinophorosaurus*, *Tornieria*, and various titanosaurs (Janensch, 1935; Hopson, 1979; Chatterjee and Zheng, 2002, 2004; Tidwell and Carpenter, 2003; Sereno et al., 2007; Witmer et al., 2008; Balanoff et al., 2010; Knoll et al., 2012, 2013; Paulina Carabajal, 2012) except for two variable features: relative proportions of the space for the venous sinus and dural peak and absence/presence of frontoparietal fenestra and postparietal foramen. In these two characters, the skull roof of *Qijianglong* is more similar to that of *Spinophorosaurus* than to those of other sauropods. Although the presence/absence of the frontoparietal fenestra and postparietal foramen individually varies within *Camarasaurus* and *Diplodocus* (Witmer et al., 2008; Knoll et al., 2012), neither of these openings has been identified in any of the skulls of *Mamenchisaurus* and *Omeisaurus* (Xing et al., 2013). Unless future discovery shows individual variation in these openings within a mamenchisaurid taxon, the presence of the postparietal foramen in *Qijianglong* is taxonomically significant.

Laterosphenoid—The left laterosphenoid (Fig. 3) is longer anteroposteriorly than tall dorsoventrally and has unfused sutures with the frontal (dorsally), orbitosphenoid (anteriorly), prootic (posteriorly), and basisphenoid (ventrally). The foramina for the oculomotor and trochlear nerves (CNs III and IV) open side by side, with the former at the laterosphenoid-basisphenoid suture. The foramen for the trigeminal nerve (CN V) sits at the laterosphenoid-prootic suture. The canal for CN V passes below this suture from the endocranial cavity to the external surface of the braincase. A foramen under a tuber anterior to the foramen of CN V may have housed the anterior middle cerebral vein.

Exoccipital and Supraoccipital—The exoccipitals and the lower half of the supraoccipital (Fig. 4) formed the lateral and dorsal margins of the foramen magnum. Unlike *Omeisaurus*, *Shunosaurus*, *Spinophorosaurus*, and cf. *Cetiosaurus* (He et al., 1988; Tang et al., 2001; Chatterjee and Zheng, 2002; Galton and Knoll, 2006; Remes et al., 2009; Knoll et al., 2012), the foramen magnum is at least twice as tall dorsoventrally as wide transversely, or may even be taller than that if fully reconstructed. Amongst sauropods, the dorsoventrally tall foramen magnum is

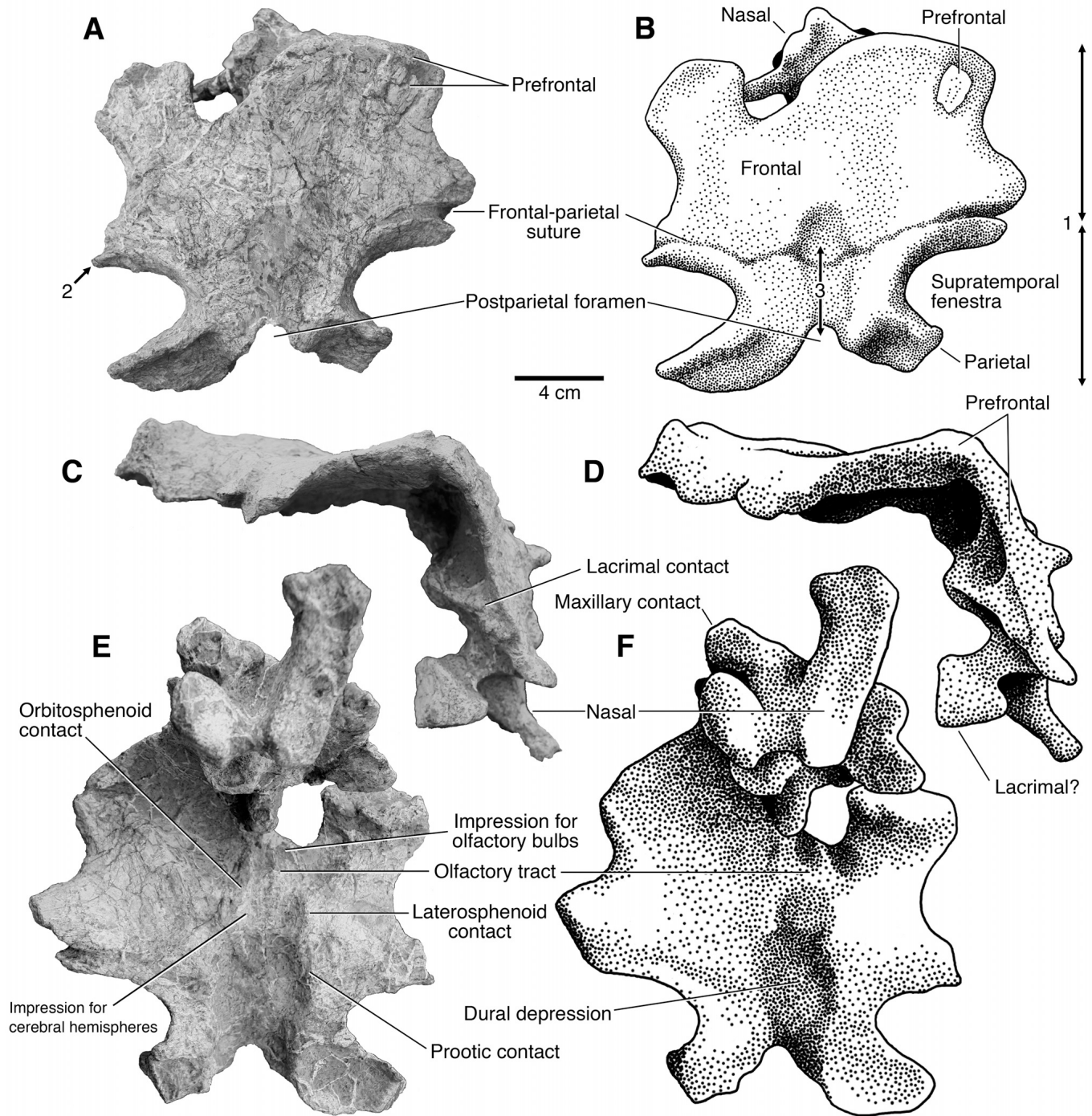


FIGURE 2. Skull roof of *Qijianglong guokr* (QJGPM 1001). **A**, photograph; **B**, interpretive drawing in dorsal view; **C**, photograph; **D**, interpretive drawing in right lateral view; **E**, photograph; **F**, interpretive drawing in ventral view. Arrow with number indicates a character diagnostic to this taxon (number refers to the list of characters in the Diagnosis).

generally a condition observed in neosauropods (both within diplodocoids and macronarians), *M. youngi*, and *Turiasaurus* (Janensch, 1935; Salgado and Bonaparte, 1991; Calvo and Salgado, 1995; Chatterjee and Zheng, 2002; Ouyang and Ye, 2002; Tidwell and Carpenter, 2003; Curry Rogers and Forster, 2004; Wilson, 2005; Wilson et al., 2005; Harris, 2006a; Paulina

Carabajal and Salgado, 2007; Garcia et al., 2008; Balanoff et al., 2010; Royo-Torres and Upchurch, 2012).

The jugular foramen and the fenestra ovalis are separated by an incomplete crista interfenestralis. The columellar canal and the groove leading to the jugular foramen extend on the anteroventral surface of the paroccipital process in parallel. The

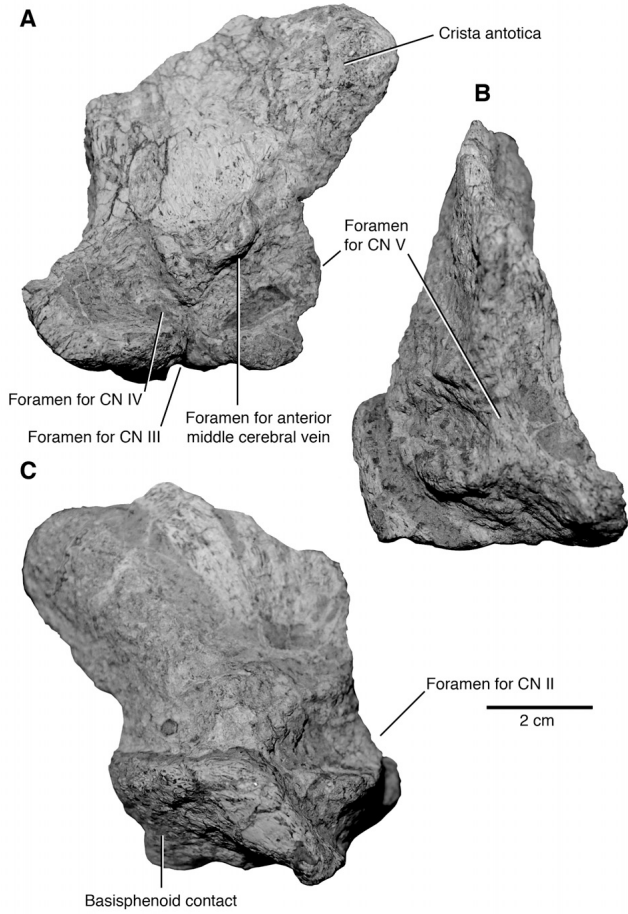


FIGURE 3. Left laterosphenoid of *Qijianglong guokr* (QJGPM 1001) in **A**, lateral view; **B**, posterior view; **C**, medial view.

incompletely fused exoccipital-opisthotic suture crosses these grooves posteroventrally. The foramen for the posterior middle cerebral vein opens below the suture with the supraoccipital. The canal for this vein passes posteriorly through a small sinus before exiting the endocranial cavity. The canal for the posterior branch of the hypoglossal nerve (CN XII) is enclosed within a depression on the medial surface of the exoccipital, just anterior to the margin of the foramen magnum. The paroccipital process is slender and without marked distal expansion.

Basioccipital, Basisphenoid, and Parasphenoid—The basicranium (Fig. 5) is nearly complete. The sutures with the laterosphenoid, prootic, opisthotic, and exoccipital are all unfused. Overall, the basicranium is dorsoventrally low and anteroposteriorly long such that the diameter of the occipital condyle is greater than the distance between the basal tuber and the base of the neck of the occipital condyle, and such that the basal tubera and the bases of the basiptyergoid process form a square in ventral view. The distance between the basal tubera is greater than the width of the occipital condyle. The craniopharyngeal foramen as described for some neosauropods (Balanoff et al., 2010) is absent. Instead, the notch between the basal tubera leads to the space between the basiptyergoid processes on the ventral surface of the basisphenoid.

The basiptyergoid process extends anteroventrally and slightly laterally. In lateral view, the extended axis of the basiptyergoid process meets the floor of the endocranial cavity at an angle of 120°, and the angle between the parasphenoid rostrum and the basiptyergoid process is accordingly smaller than perpendicular. In anterior view, the right and left basiptyergoid processes meet almost perpendicular to each other (87°). The basiptyergoid process is plate-like, not round at the end as in *Shunosaurus* (Chatterjee and Zheng, 2002). The process has an accessory tuber near the base in a direction roughly parallel with the basal tuber, which is unique to *Qijianglong* among sauropods. The crista prootica is anterodorsally oblique with respect to the floor of the endocranial cavity. Behind this crista posteriorly at midheight is a large foramen for the internal carotid artery. On the anterior side of the crista, a fossa sits around the external foramen for the abducens nerve. The parasphenoid rostrum extends more anteriorly than the basiptyergoid process, and the base of the rostrum is at the similar horizontal level with the basal tuber.

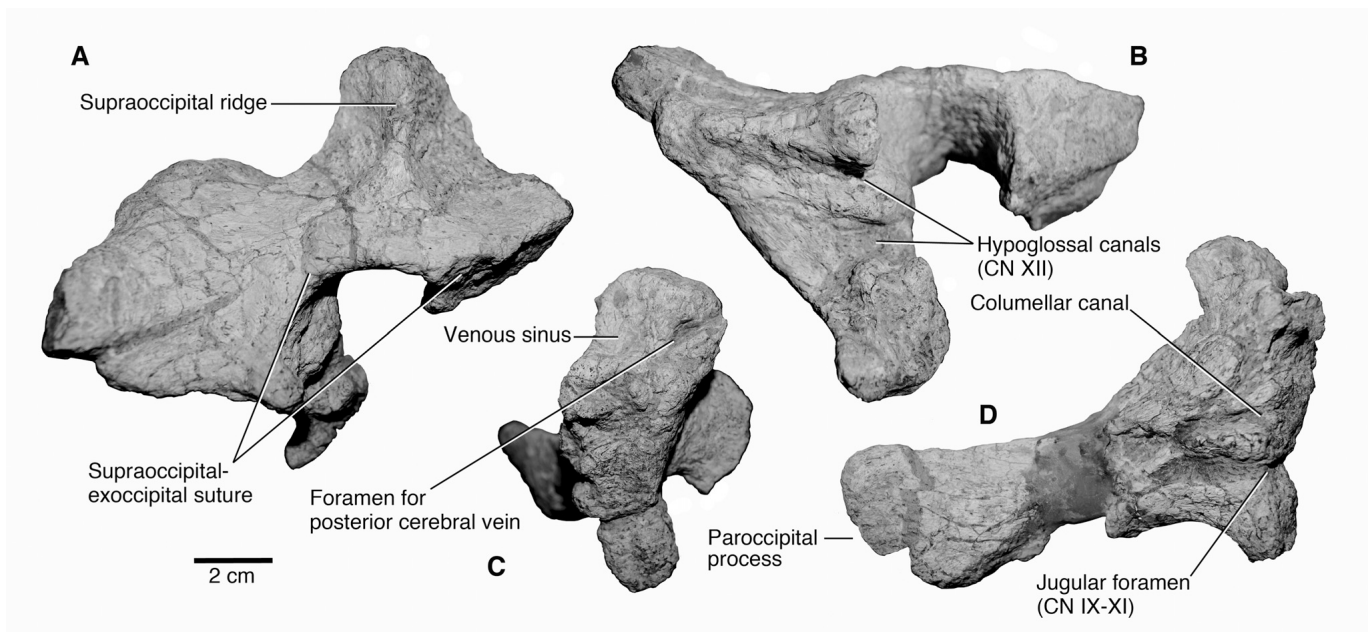


FIGURE 4. Occiput of *Qijianglong guokr* (QJGPM 1001). The supraoccipital and left exoccipital in **A**, posterior view; **B**, ventral view. The right exoccipital in **C**, anteromedial view; **D**, anterolateral view.

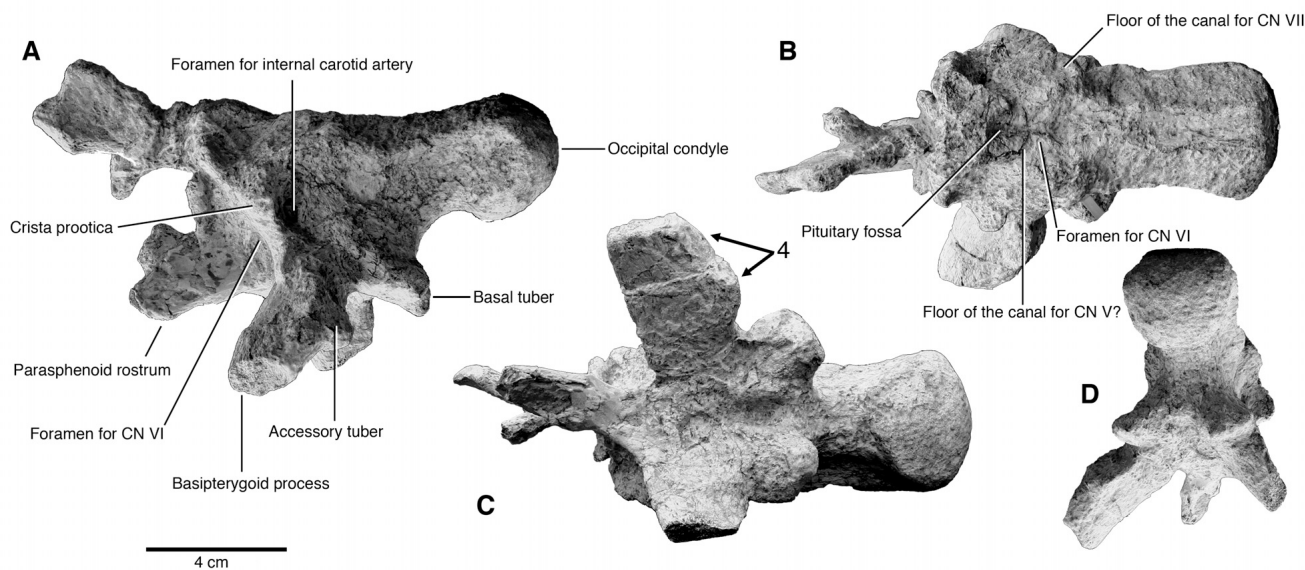


FIGURE 5. Basicranium (parasphenoid, basisphenoid, and basioccipital) of *Qijianglong guokr* (QJGPM 1001) in **A**, left lateral view; **B**, dorsal view; **C**, ventral view; **D**, posterior view. Arrow with number indicates a character diagnostic to this taxon (number refers to the list of characters in the Diagnosis).

These features of the basipterygoid process and the parasphenoid rostrum in *Qijianglong* are distinct in comparison with other basal sauropods. The basipterygoid process extends vertically and is perpendicular to both the parasphenoid rostrum and the floor of the endocranial cavity in *Chebsaurus*, *M. youngi*, *Shunosaurus*, *Turiasaurus*, and basal non-sauropod sauropodomorphs such as *Anchisaurus* and *Plateosaurus* (Galton, 1984; Benton et al., 2000; Chatterjee and Zheng, 2002; Ouyang and Ye, 2002; Läng and Mohammed, 2010; Royo-Torres and Upchurch, 2012). *Shunosaurus* also differs in that the base of the parasphenoid rostrum is lower in position than the basal tuber and that the basipterygoid processes meet at ‘U’-shape at an angle substantially broader than 90° in anterior view. In contrast, the basipterygoid process is oriented posteroventrally in parallel with the basal tuber in *Atlasaurus* and *Spinophorosaurus* as if the accessory tuber of the basipterygoid process in *Qijianglong* was greatly extended (Monbaron et al., 1999; Remes et al., 2009; Knoll et al., 2012).

In the basicranium, the canal for the trigeminal nerve (CN V) is posterior with respect to the crista prootica at the floor of the endocranial cavity. The canal for the facial nerve (CN VII) is also near the floor of the endocranial cavity and above the notch between the basipterygoid process and the basal tuber in lateral view. The broken plane intersects these two canals and represents the contact surface with the exoccipital-opisthotic, prootic, and laterosphenoid.

Prefrontal—The right prefrontal (Fig. 2) sits on the dorsal surface of the frontal and does not contact with the postorbital posteriorly. The main part of the element collapsed into the orbit. With restoration in this region, the frontal and prefrontal likely had subequal participation in the dorsal margin of the orbit. The prefrontal contacts the nasal along the medial margin, the maxilla at the anterior end, and the lacrimal at the lower end of the preorbital ramus. A fragment of the lacrimal is still attached near the contact, and the nasal sits medial to the prefrontal. This region is too weathered to make comparisons with other taxa.

Postorbital—The right postorbital (Fig. 6) is ‘T’-shaped in both lateral and dorsal views. The postorbital bar is expanded laterally such that the outline of the bone is markedly convex laterally in dorsal view. The frontal and squamosal processes are subequal in anteroposterior length. The frontal process wraps around the posterolateral corner of the frontal, whereas the

squamosal process extends posteriorly. The dorsal surface of the postorbital is nearly flat and unlike the weakly concave dorsal surface in *Omeisaurus* spp. and *Turiasaurus* (He et al., 1988; Tang et al., 2001; Royo-Torres and Upchurch, 2012). In *M.*

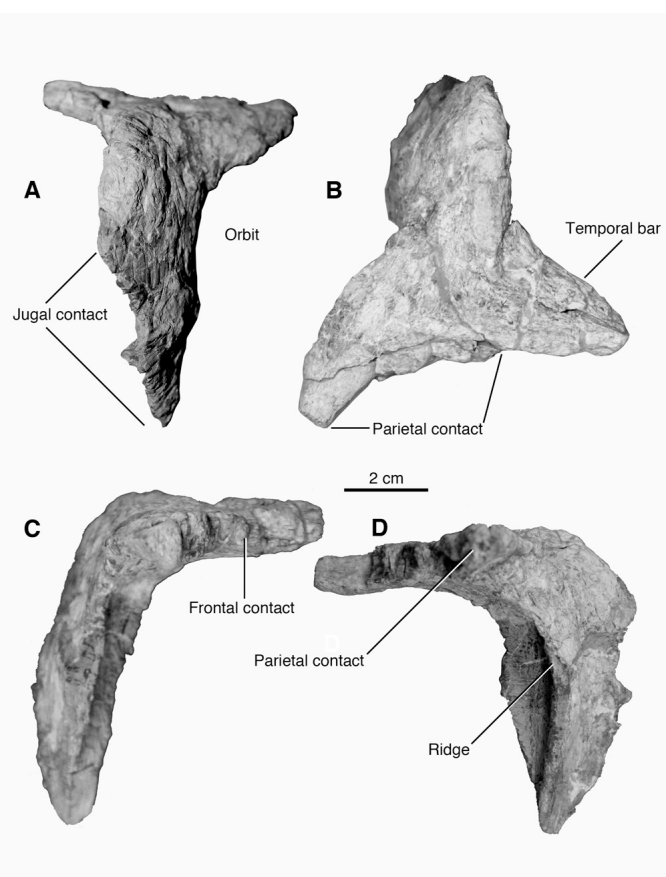


FIGURE 6. Right postorbital of *Qijianglong guokr* (QJGPM 1001) in **A**, lateral view; **B**, dorsal view; **C**, anterior view; **D**, posteromedial view.

youngi, the dorsal margin is strongly concave such that the supra-temporal fenestra is round in lateral view (Ouyang and Ye, 2002). On the medial surface of the postorbital bar, the ridge extends along the anterior margin to delineate the orbit. The jugal contacts the postorbital along the posterior margin.

Quadrate—The long axis of the right quadrate (Fig. 7) is nearly vertical as in basal eusauropods but unlike those that are inclined posterodorsally in diplodocoids and derived titanosauriforms (Upchurch et al., 2004). The shaft of the quadrate is inflated by a large pneumatic fossa as in *M. youngi* and *Turiasaurus* (Ouyang and Ye, 2002; Royo-Torres and Upchurch, 2012), whereas the fossa is shallow in *Shunosaurus* (Chatterjee and Zheng, 2002). The apex of the anteriorly expanded pterygoid ala is in the upper half of the element, whereas it is in the lower half in *O. tianfuensis* (He et al., 1988).

Pterygoid—The partial right pterygoid (Fig. 8) consists of the quadrate ala and basiptyergoid process. The quadrate ala is triangular in lateral view. The basiptyergoid process forms a shelf on the medial side of the ala as in *M. youngi* (Ouyang and Ye, 2002), rather than extending in a long process ventrally as in neosauropods such as *Dicraeosaurus* and *Giraffatitan* (Janensch, 1935). The main shaft extends anteriorly under this shelf.

Articular—The right articular (Fig. 9) has a conspicuous retroarticular process posterolateral to the articular surface with the quadrate. With the exception of the retroarticular process, the lateral surface of the articular was overlapped by the surangular (not preserved). The medial surface of the articular has a fossa within which the posterior end of the prearticular (not preserved) fit. The articular surface has a shallow profile, with slight concavity in lateral view.

Postcranial Skeleton

Nomenclature for the vertebral laminae and pneumatic fossae follows Wilson (1999) and Wilson et al. (2011), respectively.

Cervical Vertebrae—The completely preserved cervical series of *Qijianglong* consists of 17 vertebrae (Figs. 10–12). The axis to

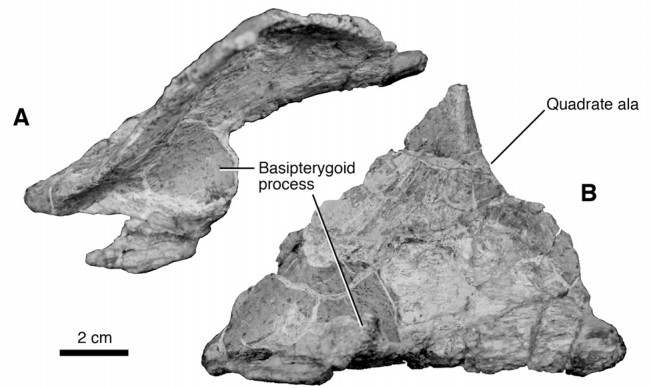


FIGURE 8. Right pterygoid of *Qijianglong guokr* (QJGPM 1001) in **A**, dorsal view; **B**, medial view.

the 11th cervical vertebra were fully articulated in the quarry. The atlas intercentrum and the 12th–17th cervical vertebrae were closely associated with the series. Except for the amphicoelous atlas intercentrum, the cervical vertebrae are all opisthocelous. Overall, the anterior cervical vertebrae (3rd–5th) have relatively anteroposteriorly elongate centra in *Qijianglong* that are typically more than three times as long as high (Supplementary Data, Table S1). The relative centrum length in this region

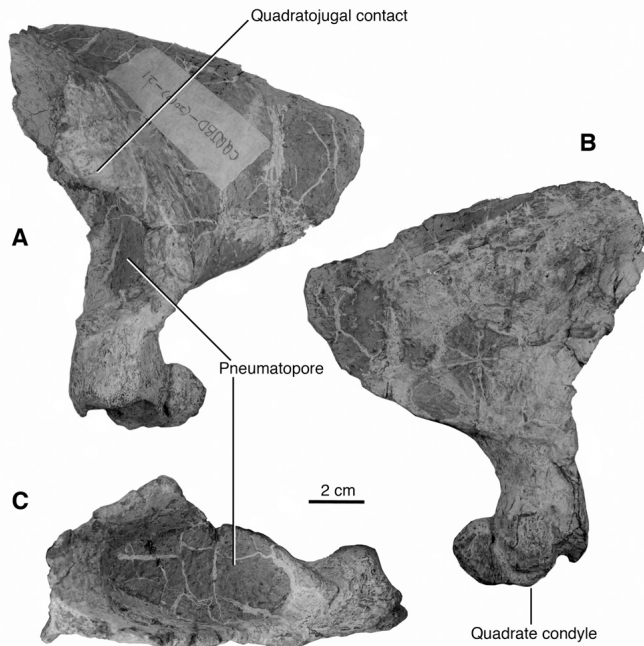


FIGURE 7. Right quadrate of *Qijianglong guokr* (QJGPM 1001) in **A**, lateral view; **B**, medial view; **C**, posterior view, rotated 90° counterclockwise.

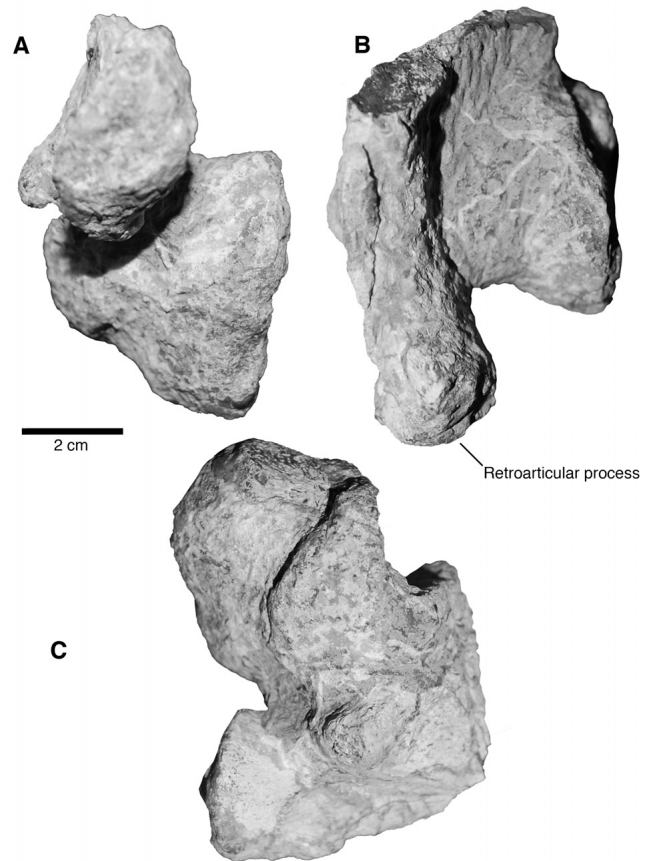


FIGURE 9. Right articular of *Qijianglong guokr* (QJGPM 1001) in **A**, lateral view; **B**, dorsal view; **C**, ventral view.

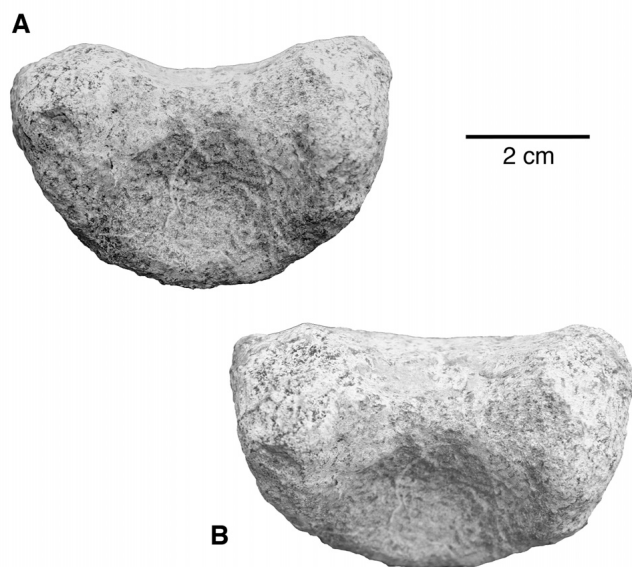


FIGURE 10. Atlas intercentrum of *Qijianglong guokr* (QJGPM 1001) in **A**, anterior view; **B**, posterior view.

of the cervical series is greater in this taxon than in *Chuanjiesaurus*, *M. anyuensis*, *M. hochuanensis*, *M. sinocanadorum*, and *Tonganosaurus* and is roughly comparable to *M. youngi* and *O. tianfuensis* (Table S1; Russell and Zheng, 1993; He et al., 1996; K. Li et al., 2010b; Sekiya, 2011).

The semilunar atlas intercentrum (Fig. 10) contacts the odontoid process of the axis posteroventrally (Fig. 11A). The anterior articular surface of the axis is rugose and flat, indicating an incompletely fused contact with the atlas intercentrum. The planar spinous process of the axis extends over the dorsomedially oriented spinopostzygapophyseal lamina. As a result, the spinopostzygapophyseal fossa forms a deep recess closed dorsally by the spinous process. The posterior centrodiapophyseal lamina is incomplete. The diapophysis is more anterior than the longitudinal midpoint of the centrum and extends from the edge of the anterior articular surface via the anterior centrodiapophyseal lamina. The prezygodiapophyseal lamina is incomplete and not directly connected to the diapophysis. The axis has three pleurocoels on the right side and two on the left. On the right side, each pleurocoel is round and successively smaller posteriorly. On the left side, the anterior pleurocoel is more than double the area of the posterior one. The pleurocoels on the left side are anteroposteriorly elongate.

In the anterior to mid-cervical region (Fig. 11B–H), the spinous process forms a longitudinal plate that is split posteriorly into the bilaterally paired spinopostzygapophyseal laminae in all of the 6th–8th vertebrae. The lamina is oriented primarily anterodorsally such that the spinopostzygapophyseal fossa is open dorsally. The spinodiapophyseal fossa is a shallow depression. In lateral view, the prezygodiapophyseal lamina overhangs the centrum and overlaps the postzygapophysis of the previous vertebra from lateral side. The posterior centrodiapophyseal lamina extends posteriorly in a straight line to the base of the neural arch, thereby separating the postzygapophyseal centrodiapophyseal fossa from the deeply excavated centrodiapophyseal fossa. This lamina is clearly more pronounced than the postzygodiapophyseal lamina in the anterior cervical series in *Qijianglong*, and possibly in *M. sinocanadorum*, whereas this condition is typically reversed in other mamenchisaurids, including *Chuanjiesaurus*, *M. youngi*, *Omeisaurus* spp., and *Tonganosaurus* (He et al.,

1988; Russell and Zheng, 1993; Tang et al., 2001; Ouyang and Ye, 2002; Sekiya, 2011). The postzygodiapophyseal lamina originates from the posterior centrodiapophyseal lamina posterodorsal to the diapophysis. The postzygodiapophyseal lamina is prominent enough in the mid-cervical region (from the 5th/6th onward) to overhang the centrum and extend posteriorly beyond the posterior articular surface as in *Chuanjiesaurus*, but unlike *Mamenchisaurus* spp., *Omeisaurus* spp., and *Tonganosaurus* (He et al., 1988; Russell and Zheng, 1993; Tang et al., 2001; Ouyang and Ye, 2002; K. Li et al., 2010b; Sekiya, 2011). The maximum vertical height of the postzygapophysis is twice that of the spinous process. The zygapophyses articulate with one another at the level slightly above the centrum in the 7th and 8th, but at a level noticeably higher above the centrum in the 6th cervical vertebra. Although the centropostzygapophyseal fossa is not visible in lateral view, it forms a deep pit set between the prominent centropostzygapophyseal lamina and the postzygapophysis in the 8th cervical vertebra. This fossa is absent in the 6th cervical vertebra in which the postzygapophysis is raised high above the level of the centrum.

In the 12th–14th cervical vertebrae of the posterior cervical region (Fig. 12A–C), the postzygodiapophyseal lamina originates above the posterior centrodiapophyseal lamina as in the cervical vertebrae of *Chuanjiesaurus*, *M. youngi*, and *Omeisaurus* spp. (He et al., 1988, 1996; Tang et al., 2001; Ouyang and Ye, 2002; Sekiya, 2011), not from the latter lamina as in the more anterior or posterior cervical vertebrae. The postzygapophysis is well above the centrum. The 17th cervical vertebra is the last of the cervical series (Fig. 12F) as in *Omeisaurus*. The neural arch is relatively taller than in the more anterior cervical vertebrae. The spinous process is as tall as the centrum, and the both zygapophyses articulated well above the centrum. On the left side of the process, the spinodiapophyseal fossa has three pneumatopores. There are at least seven, and likely more, pneumatopores within the fossa on the right side of the spinous process. The prezygapophysis is pneumatic and associated with a tubercle along the anterior margin. Other posterior cervical vertebrae also have pneumatopores in the spinous process, whereas the pneumatopores are absent in other mamenchisaurids such as *Chuanjiesaurus*, *M. youngi*, and *Omeisaurus* spp. (He et al., 1988, 1996; Tang et al., 2001; Ouyang and Ye, 2002; Sekiya, 2011)

From the axis to at least the 14th cervical vertebra, a finger-like process extends posteriorly above the postzygapophysis and overlaps onto the dorsolateral surface of the prezygapophysis of the next vertebra (Fig. 11I, J). These processes are unique to *Qijianglong*, unlike all previously known mamenchisaurids that are preserved with cervical vertebrae (e.g., *Chuanjiesaurus*, *Mamenchisaurus* spp., *Omeisaurus* spp., *Tonganosaurus*). Therefore, the neck of *Qijianglong* presumably had a range of motion restricted in sideways.

Dorsal Vertebrae—Six dorsal vertebrae are preserved from the anterior thoracic region (Fig. 13). Although posterodorsal crushing makes comparison difficult, the vertebrae likely represent the 1st–6th dorsals. These vertebrae are all opisthocoelous and generally identical in morphology except for a dorsal shift in position of the parapophysis posteriorly along the series. Based on the better-preserved 3rd–6th vertebrae, the centra are more strongly opisthocoelous rather than nearly amphiplatyan as in *Eomamenchisaurus* (Lü et al., 2008). The centra are anteroposteriorly longer than dorsoventrally tall as in *Mamenchisaurus* spp. and *Xinjiangtitan*, but unlike *Chuanjiesaurus*, *Eomamenchisaurus*, *Omeisaurus* spp., *Tonganosaurus*, and *Yuanmousaurus* (He et al., 1988, 1996; Tang et al., 2001; Ouyang and Ye, 2002; Lü et al., 2006, 2008; K. Li et al., 2010b; Sekiya, 2011; Wu et al., 2013). The neural arches with the spinous processes are at least 1.5 times the height of the centra. The bifurcated spinous processes of *Qijianglong* differ from those of *Hudiesaurus* in lacking the medial projections between the bifurcate processes (Dong, 1997).

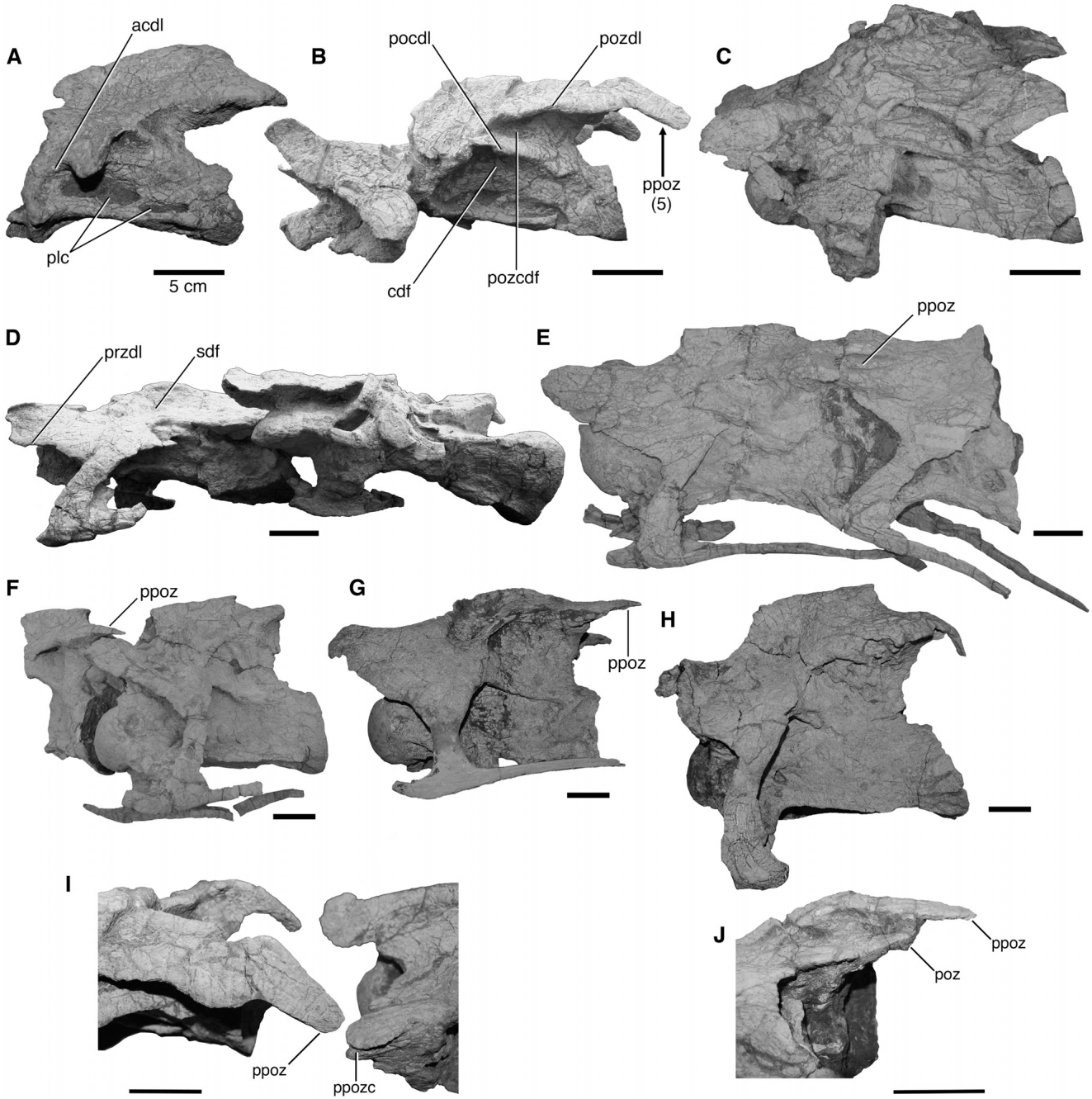


FIGURE 11. Anterior cervical series of *Qijianglong guokr* (QJGPM 1001) in left lateral views unless otherwise noted. **A**, axis; **B**, cervical vertebra 3; **C**, cervical vertebra 4; **D**, cervical vertebrae 5 and 6; **E**, cervical vertebra 7 and anterior half of cervical vertebra 8 (horizontally inverted; showing right side); **F**, posterior half of cervical vertebra 8 and cervical vertebra 9; **G**, cervical vertebra 10; **H**, cervical vertebra 11; **I**, close-up of the prezygapophysis-postzygapophysis contact between cervical vertebrae 3 and 4 in dorsolateral view, showing finger-like process lateral to postzygapophysis; **J**, close-up of the postzygapophysis of cervical vertebra 5 in dorsal view, showing finger-like process lateral to postzygapophysis. Arrow with number indicates a character diagnostic to this taxon (number refers to the list of characters in the Diagnosis). All scale bars equal 5 cm. **Abbreviations:** **acdl**, anterior centrodiapophyseal lamina; **cdf**, centrodiapophyseal fossa; **plc**, pleurocoel; **pocdl**, postcentrodiapophyseal lamina; **poz**, postzygapophysis; **pozcdf**, postzygapophyseal centrodiapophyseal fossa; **pozdl**, postzygodiapophyseal lamina; **ppoz**, finger-like process lateral to postzygapophysis; **ppozc**, groove for contact with finger-like process; **przd**, prezygodiapophyseal lamina; **sdf**, spinodiapophyseal fossa.

Based on the 3rd–6th dorsal vertebrae, the prezygapophyseal centrodiapophyseal fossa extends onto the anterior surface of the transverse process with four distinct pneumatopores, whereas the fossa is smooth in other mamenchisaurids such as

M. youngi (Ouyang and Ye, 2002). The centrodiapophyseal fossa is a low triangular depression with a pleurocoel tucked underneath the transverse process. The postzygapophyseal centrodiapophyseal fossa occupies about three times the area of the

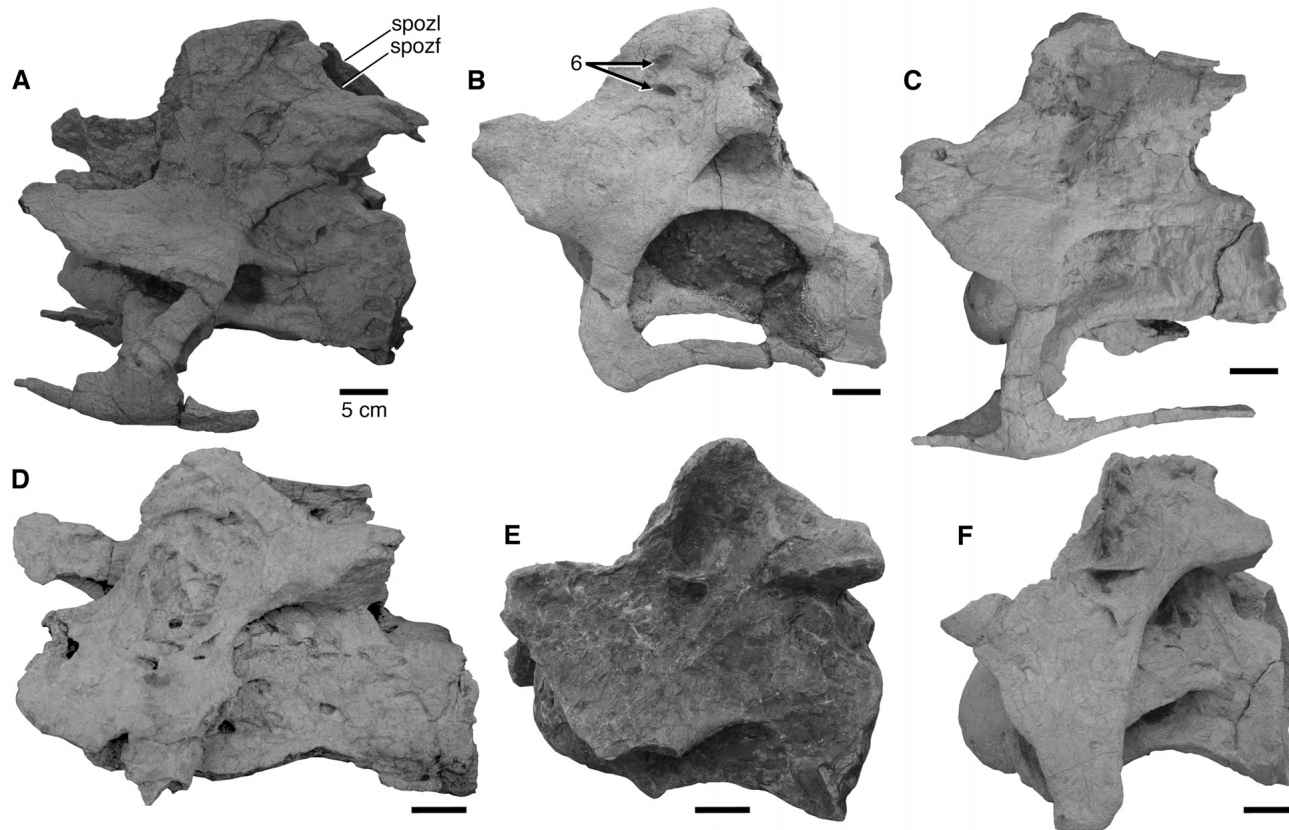


FIGURE 12. Posterior cervical series of *Qijianglong guokr* (QJGPM 1001) in left lateral view unless otherwise noted. **A**, cervical vertebra 12; **B**, cervical vertebra 13; **C**, cervical vertebra 14; **D**, cervical vertebra 15 (horizontally inverted; showing right side); **E**, cervical vertebra 16 (horizontally inverted; showing right side); **F**, cervical vertebra 17 (horizontally inverted; showing right side). Arrow with number indicates a character diagnostic to this taxon (number refers to the list of characters in the Diagnosis). All scale bars equal 5 cm. **Abbreviations:** **spozf**, spinopostzygapophyseal fossa; **spozi**, spinopostzygapophyseal lamina.

prezygapophyseal centrodiapophyseal fossa in lateral view. This condition is similar to that of *O. tianfuensis* and *Tonganosaurus* (He et al., 1988; K. Li et al., 2010b). In other mamenchisaurids such as *Chuanjiesaurus*, *Mamenchisaurus* spp., and *Yuanmousaurus* (He et al., 1996; Ouyang and Ye, 2002; Lü et al., 2006; Sekiya, 2011), the latter fossa is typically larger than the former.

The upper half of the postzygapophyseal centrodiapophyseal fossa is separated into two chambers by a vertical lamina descending from the spinopostzygapophyseal lamina. The anterior of the two chambers represents an incipient postzygapophyseal spinodiapophyseal fossa. The postzygapophyseal centrodiapophyseal fossa has a pneumatopore at the

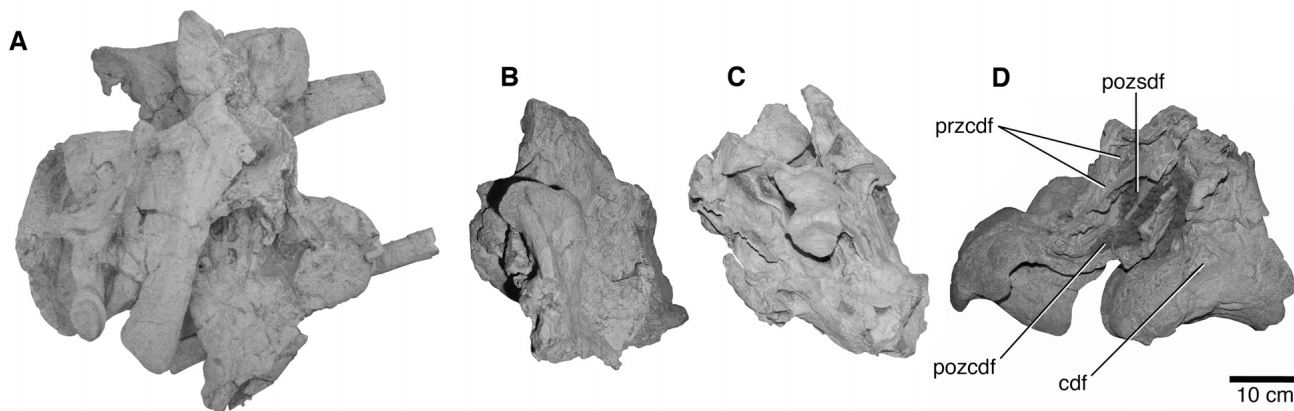


FIGURE 13. Dorsal series of *Qijianglong guokr* (QJGPM 1001). The dorsal vertebrae are crushed dorsoventrally or transversely. **A**, dorsal vertebra 1 (dorsoventrally crushed) in dorsal view; **B**, incomplete dorsal vertebra 2 in left lateral view; **C**, dorsal vertebrae 3 and 4 in lateral view (horizontally inverted; showing right side); **D**, dorsal vertebrae 5 and 6 in left lateral view. **Abbreviations:** **cdf**, centrodiapophyseal fossa; **pozcdf**, postzygapophyseal centrodiapophyseal fossa; **pozsdf**, postzygapophyseal spinodiapophyseal fossa; **przcdf**, prezygapophyseal centrodiapophyseal fossa.

dorsomedial corner in posterior view. The right and left counterparts of the fossa are set apart by a vertical ridge below the spinopostzygapophyseal fossa.

Caudal Vertebrae—The caudal series is represented by 28 vertebrae (Fig. 14). Although the precise identification is difficult, these vertebrae are from the middle to distal region of the tail. One caudal centrum is procoelous and the other centra are amphiplatyan.

Based on comparisons with *Mamenchisaurus* spp. and *Omeisaurus* spp. (He et al., 1988; Tang et al., 2001; Ouyang and Ye, 2002), the procoelous centrum is from around the 10th caudal positions. The posterior articular surface is convex for only 16% of the diameter of the centrum. There is no pneumatic fossa on the lateral surface of the centrum. The ventral surface of the centrum has a longitudinal sulcus on the posterior half. The prezygapophysis extends anterodorsally, and its distal tip is slightly beyond the anterior articular surface of the centrum. The spinoprezygapophyseal lamina is a simple low ridge on the dorsal half of the spinous process. The transverse process has no centrodiapophyseal laminae. The spinous process is inclined posterodorsally at approximately 75°.

The rest of the caudal vertebrae are from the middle to distal caudal series (from the 15th onward). The spinous process and the postzygapophysis are inclined posterodorsally beyond the centrum and over half the length of the next centrum as in *Mamenchisaurus* spp. (Ouyang and Ye, 2002). The most distal two of the preserved caudal vertebral centra are fused to each other (Fig. 13G). The fusion is possibly pathologic.

Pubis—The left pubis (Fig. 15) is transversely flat and vertically tall and has a vertically elongate inverted teardrop-shape in cross-section. The anterior margin is deeply concave such that the distal end of the pubis points more anteriorly than ventrally in life position, whereas the general condition amongst sauropods is a distal end of a pubis oriented more ventrally than anteriorly. The pubic foramen is enclosed within the peduncle for the ischial contact, and the flange extends along the ventral margin for half the length of the shaft. This suite of traits differs from *Eomamenchisaurus*, *M. youngi*, and *O. maoianus* in being more

robust, from *Chuanjiesaurus* in having a pubic foramen, from *O. tianfuensis* in having a clearly demarcated, concave acetabular margin, and from *Xinjiangtitan* in lacking a marked constriction proximal to the pubic apron (He et al., 1988; Tang et al., 2001; Ouyang and Ye, 2002; Lü et al., 2008; Sekiya, 2011; Wu et al., 2013).

Other Postcranial Elements—The dorsal ribs are preserved in fragments, with a pneumatopore at the base of the capitulum. The hemal arches from the mid-caudal positions are closed dorsally by a bony bridge between the right and left articular facets, whereas the arches from the distal caudal positions are open. Both of the two pedal phalanges represent the proximal phalanx of each digit, but the precise identification of the digits is uncertain.

PHYLOGENETIC ANALYSIS

A maximum parsimony analysis used the data set of Harris (2006b), with modifications by Xing et al. (2013) and the addition of *Qijianglong* (Supplementary Data, Appendix S1). In this matrix, 'Prosauropoda' were split into *Plateosaurus* and *Thecodontosaurus*. *Mamenchisaurus* and *Omeisaurus* were split into multiple species for which information is available from the literature and the authors' collections visits: *M. anyuensis*, *M. constructus*, *M. hochuanensis*, *M. sinocanadorum*, *M. youngi*, *O. maoianus*, and *O. tianfuensis* (Young, 1958; Young and Zhao, 1972; He et al., 1988, 1996; Russell and Zheng, 1993; Tang et al., 2001; Ouyang and Ye, 2002). The following taxa were added to Harris's (2006b) data set: *Atlasaurus*, *Chuanjiesaurus*, *Lirainosaurus*, *Nebulasaurus*, *Spinophorosaurus*, *Tornieria*, *Turiasaurus*, and *Yuanmousaurus* (Monbaron et al., 1999; Sanz et al., 1999; Lü et al., 2006; Remes, 2006; Royo-Torres et al., 2006; Remes et al., 2009; Díaz et al., 2011; Sekiya, 2011; Knoll et al., 2012; Royo-Torres and Upchurch, 2012; Xing et al., 2013). Harris's (2006b) characters 38 and 76 were modified, and 13 braincase characters were added (Xing et al., 2013). Character codes for individual taxa were extensively modified to follow recently added information in the literature. For the current data set, scorings were modified for *Barapasaurus*, *Brachiosaurus*,

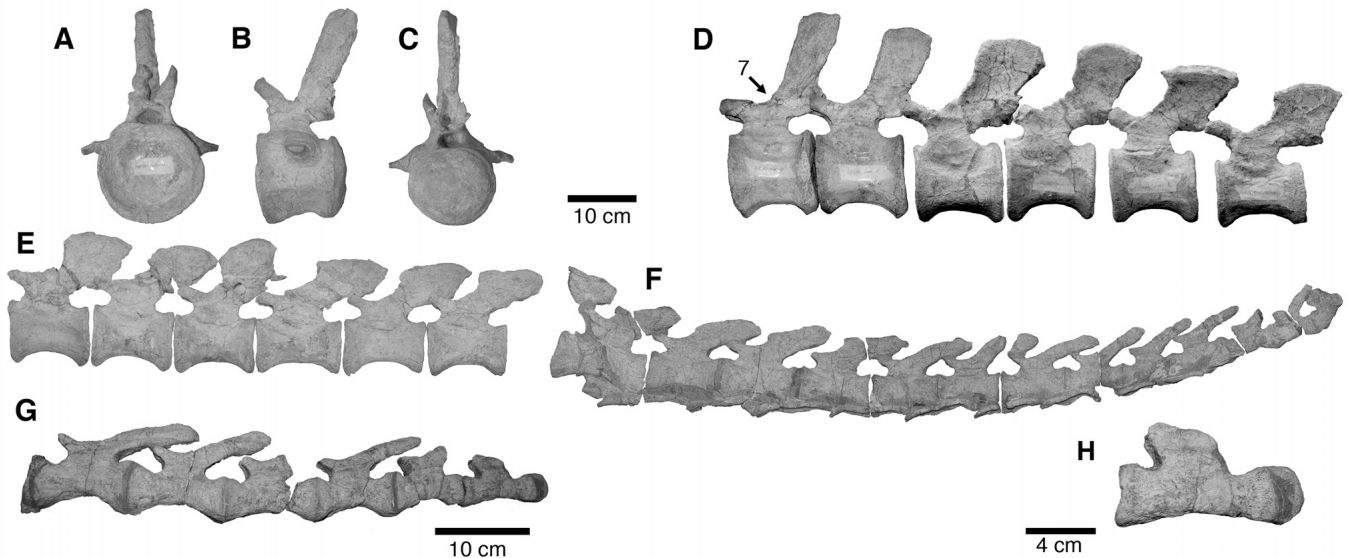


FIGURE 14. Caudal series of *Qijianglong guokr* (QJGPM 1001). A mid-caudal vertebra in **A**, anterior view; **B**, left lateral view; **C**, posterior view. Distal caudal series in left lateral view: **D**, possible caudal vertebrae 15–20; **E**, possible caudal vertebrae 21–26; **F**, possible caudal vertebrae 27–39; **G**, close-up photograph of possible caudal vertebrae 35–41; **H**, close-up photograph of possible caudal vertebrae 40 and 41. The centrum of the caudal vertebra 41 is fused to that of the caudal vertebra 40. Arrow with number indicates a character diagnostic to this taxon (number refers to the list of characters in the Diagnosis).

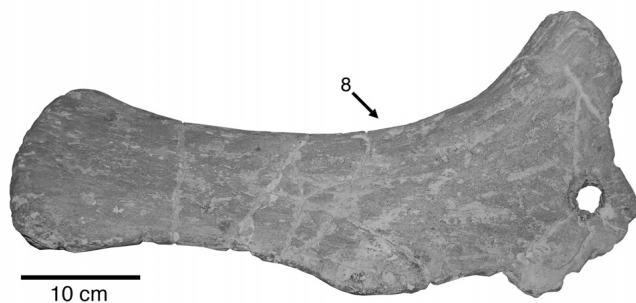


FIGURE 15. Left pubis of *Qijianglong guokr* (QJGPM 1001) in lateral view. Arrow with number indicates a character diagnostic to this taxon (number refers to the list of characters in the Diagnosis).

Nigersaurus, and *Euhelopus* following Sereno et al. (2007), Taylor (2009), Wilson and Upchurch (2009), Nair and Salisbury (2012), and Poropat and Kear (2013). The following changes were made based on personal communications from J. D. Harris (pers. comm., 2012): *Camarasaurus* (characters 101–149 as missing ‘?’); *Limaysaurus* (character 319 from ‘2’ to ‘?’); and *Nemegtosaurus* (characters 301–305 as missing ‘?’). The following characters were parsimony uninformative and therefore removed from the analysis: 40, 47, 89, 136, 271, and 336. The current data set includes 45 taxa (including three outgroups: Theropoda, *Plateosaurus*, and *Thecodontosaurus*) and 338 characters. All characters were treated as unordered.

A heuristic search by PAUP b.4.01 (Swofford, 2003) with multiple TBR + TBR search strategy recovered more than 29,500 most parsimonious trees (MPTs; tree length [TL] = 1056; consistency index [CI] = 0.400; retention index [RI] = 0.643; rescaled consistency index [RC] = 0.257). A strict consensus of all MPTs (Fig. 16A) supports a monophyletic Mamenchisauridae, with *O. tianfuensis* as the sister taxon to the rest of the clade, and with *Chuanjiesaurus* and *Qijianglong* nested outside a polytomy including *Mamenchisaurus* spp., *O. maolianus*, and *Yuanmousaurus*. *Qijianglong* therefore represents a mamenchisaurid lineage that extends back at least to the Middle Jurassic and is not the closest relative of *M. anyuensis*, which occurs in the upper part of the same formation. This result also provides the first phylogenetic support for the mamenchisaurid affinity of *Yuanmousaurus*, which was originally compared with *Patagosaurus* (Lü et al., 2006). Coupled with the undiagnosable nature of the holotype (Xing et al., 2013), *Yuanmousaurus* cannot be readily distinguished from *Eomamenchisaurus* from the same Zhanghe Formation on the basis of the available information (Lü et al., 2008). Although this paper accepts the priority of *Eomamenchisaurus* over *Yuanmousaurus* because of the undiagnostic nature of the latter, these two genera await further detailed description of the type materials and taxonomic revision.

In the second round of the heuristic search under the same setting, *M. sinocanadorum* and *Yuanmousaurus* were removed from the analysis. Scored characters for *M. sinocanadorum* have no overlap with those of the type species of *Mamenchisaurus*, *M. constructus*, in the data matrix. This second analysis recovered 542 MPTs (TL = 1046; CI = 0.403; RI = 0.644; RC = 0.260). A strict consensus of the MPTs partly resolves the polytomy of *Mamenchisaurus* spp. and *O. maolianus* and is identical to the strict consensus of the whole data set in the rest of the tree

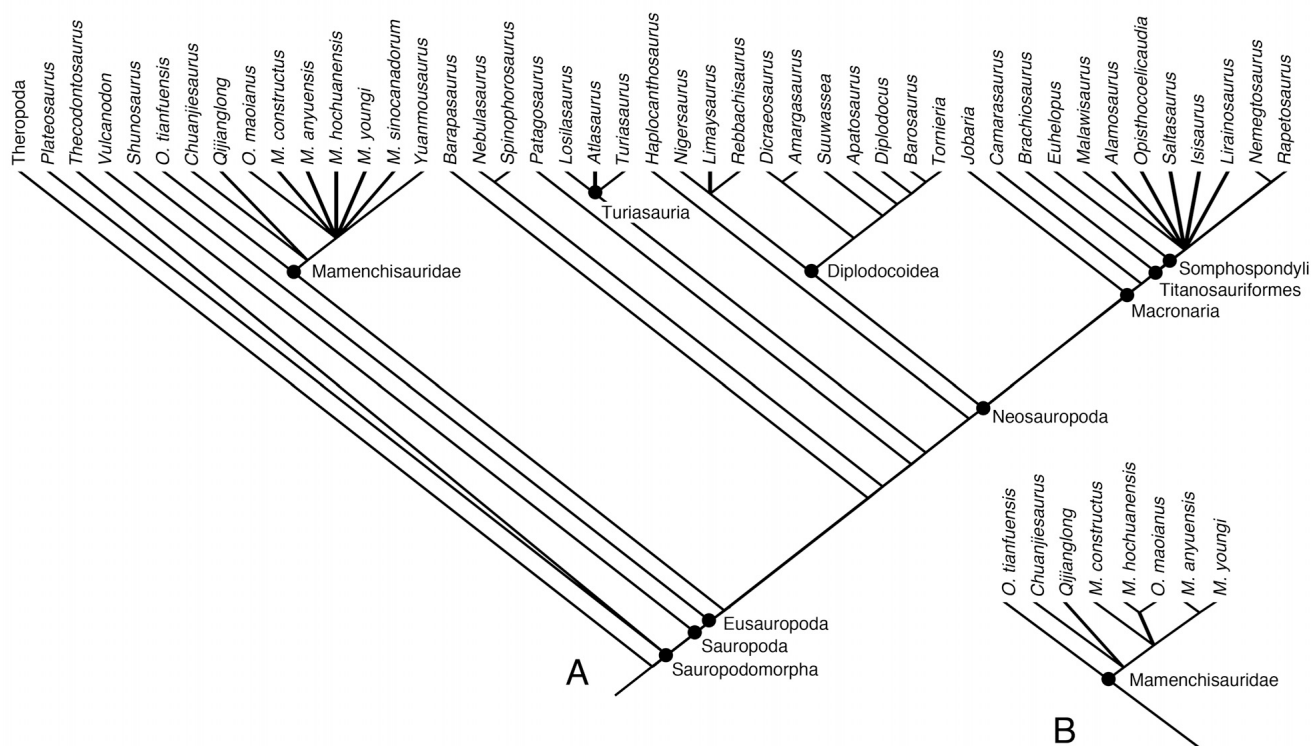


FIGURE 16. Results of maximum parsimony analyses for *Qijianglong* and its relationships to other sauropods. **A**, strict consensus of shortest trees from a maximum parsimony analysis of 45 taxa including *Qijianglong guokr* based on the data set modified from Harris (2006b) (see Supplementary Data); **B**, a part of strict consensus of shortest trees using the same data set without *Mamenchisaurus sinocanadorum* and *Yuanmousaurus*. The mamenchisaurid interrelationships are better resolved, and the rest of the tree is identical to **A**. See text for description of the trees, tree statistics, and discussion.

(Fig. 16B). Each of the pairs *M. hochuanensis* + *O. maoianus* and *M. youngi* + *M. anyuensis* forms a clade, and these two clades and *M. constructus* form a polytomy.

In both analyses, the Mamenchisauridae sits in a relatively basal position, more derived than *Shunosaurus* but outside of the rest of eusauropods. The clade is supported by 10 unambiguous character changes in each of the analyses, but the supporting character changes slightly differ between the two (*analysis 1; **analysis 2; '0' to '1' for characters 64**, 100, 102, 110, 144, 146, 148, 307, 337*; '1' to '2' for character 126; '1' to '2' for character 126; '4' to '6' for character 105). These characters are sagittal and transverse nuchal crests merging smoothly (character 64); denticles absent on distal margin of tooth (100); procumbent teeth (102); more than 15 cervical vertebrae (105); fossa above parapophysis of cervical vertebra confluent with lateral pneumatic fossa (110); hypantrum-hyposphene contact in dorsal vertebrae (126); spinopostzygapophyseal lamina unconnected to postspinal lamina in posterior dorsal vertebra (144); spinodiapophyseal and spinopostzygapophyseal laminae contacting each other in posterior dorsal vertebra (146); moderate triangular process at distal end of neural spine on dorsal vertebra (148); ossified calcaneum absent (307); and supraoccipital wider transversely than tall vertically (337).

The clade of mamenchisaurids with the exclusion of *O. tianfuensis* is supported by six unambiguous character changes in both analyses ('0' to '1' for characters 28, 150, 166, 168, 207; '2' to '3' in character 143). These characters are frontal-parietal suture anterior to supratemporal fenestra (28); prespinal and spinoprezygapophyseal lamina connected in posterior dorsal vertebra (143); opisthocelous posterior dorsal vertebra (150); procoelous first and proximal caudal vertebrae (166, 168); and dorsal-most point of acromion process posteriorly displaced (207).

Further internal nodes within the Mamenchisauridae are supported by two characters each. The polytomy of *Mamenchisaurus* spp. and *O. maoianus* in the second analysis is characterized by characters 156 ('1' to '2'; five sacral vertebrae) and 169 ('0' to '2'; transversely compressed articular surface of proximal caudal vertebra). The clade of *M. hochuanensis* and *O. maoianus* is supported by '0' to '1' unambiguous changes in characters 248 and 294 (longest metacarpal about 35% to 45% the length of radius; tibia transversely twice wider at distal condyle as at midshaft). The clade of *M. anyuensis* and *M. youngi* is supported by '0' to '1' unambiguous changes in characters 225 and 287 (proximolateral process of humerus reduced; distal condyle for tibia more than twice wider than that for fibula in femur).

DISCUSSION AND CONCLUSION

Qijianglong is a significant addition to the Asian fossil record of sauropods because it is the first mamenchisaurid definitively distinct from *Mamenchisaurus* spp. from the Late Jurassic of China. Not only does it increase the generic diversity of mamenchisaurids from that time interval, but the seemingly derived morphology of *Qijianglong* and the basal phylogenetic position of mamenchisaurids suggests that mamenchisaurids independently evolved conditions convergent with other sauropods. The postparietal foramen is absent in other mamenchisaurids but widespread among eusauropods. The presence of an accessory tuber of the basiptyergoid process extending in parallel with the basal tuber is unique among sauropods. The closest condition occurs in *Atlasaurus* and *Spinophorosaurus* in which the basiptyergoid process extends in parallel with the basal tuber. The extensive pneumatization of the cervical vertebrae is unlike other mamenchisaurids and reminiscent of diplodocoids.

The geographic isolation of Asia in Late Jurassic times (Russell, 1993; Barrett and Upchurch, 2005; Mannion et al., 2011) could explain both the low diversity of sauropodomorphs

and the convergent morphology of *Qijianglong* with distantly related sauropods. During this time interval in Asia mamenchisaurids are currently the sole sauropods (Table 1). The low species richness of mamenchisaurids from the Late Jurassic of Asia may be attributed to a smaller number of fossiliferous terrestrial localities than for preceding time intervals. However, the parsimony analysis presented in this paper (Fig. 16) indicates that both basal and derived lineages of mamenchisaurids existed in Late Jurassic times. As such, mamenchisaurids do not appear to have gone through a bottleneck across the Middle–Late Jurassic boundary. Current evidence suggests that sauropod lineages other than mamenchisaurids did not survive into Late Jurassic times. This endemic sauropod fauna in the Late Jurassic of Asia was replaced by titanosauriforms across the Jurassic–Cretaceous boundary.

A surprising result of the parsimony analysis was the relatively basal position of mamenchisaurids (Fig. 16). In previous analyses, *Mamenchisaurus* and *Omeisaurus* are typically recovered as relatively derived non-neosauropod eusauropods, often just outside the Neosauropoda (Harris, 2006b; Royo-Torres et al., 2006, 2009; Remes et al., 2009; Läng and Mahammed, 2010; Sekiya, 2011; Nair and Salisbury, 2012; Royo-Torres and Upchurch, 2012). Instead, the current analysis suggests that mamenchisaurids represent an ancient lineage of basal eusauropods only slightly more derived than *Shunosaurus*. This basal position is consistent with the Early Jurassic age of the putative mamenchisaurid *Tonganosaurus* (K. Li et al., 2010b).

The analysis also recovered a monophyletic Mamenchisauridae and subclades within the lineage (Fig. 16). Mamenchisauridae can be defined as a stem-based clade more closely related to *M. constructus*, *M. youngi*, *O. junghsiensis*, and *O. tianfuensis* than to *Shunosaurus*, *Barapasaurus*, *Patagosaurus*, or *Spinophorosaurus*. This result contradicts the recovery of Mamenchisauridae excluding *Omeisaurus* as proposed by Sekiya (2011). In further comparison with Sekiya's (2011) analysis, *Mamenchisaurus* spp. form a paraphyletic assemblage in the present analysis as opposed to a polyphyletic assemblage, and *Chuanjiesaurus* is nested outside the '*Mamenchisaurus*' polytomy as opposed to being found in a derived position as the sister taxon to *M. hochuanensis*. These differences of opinion regarding mamenchisaurid interrelationships highlight the need for a taxonomic revision of *Mamenchisaurus* and *Omeisaurus*. Taken at face value, the present analysis suggests that (1) *O. maoianus* and *O. tianfuensis* are likely not congeneric; (2) the genus *Mamenchisaurus* should be restricted to the type species, *M. constructus*, because of the poorly resolved relationships among derived mamenchisaurids; and (3) each of the '*Mamenchisaurus*' clades (*M. hochuanensis* + *O. maoianus*; *M. anyuensis* + *M. youngi*), if tested positive, represent distinct lineages. However, this analysis does not include the type species *O. junghsiensis*, other described species of *Mamenchisaurus* and *Omeisaurus*, and newly described mamenchisaurids such as *Eomamenchisaurus*, *Tonganosaurus*, and *Xinjiangtitan* (Lü et al., 2008; K. Li et al., 2010b; Wu et al., 2013). These taxa were omitted from the analysis because published information was not sufficient, because the authors have not examined the materials, or because their inclusion was not justified like other highly incomplete taxa (e.g., *Yuanmousaurus*, *M. constructus*) that are crucial for tests of taxonomic validity. Therefore, it remains uncertain whether or not some species might turn out to be synonyms, and whether either or neither of the two species of *Omeisaurus* included in the analysis better represents that genus.

A mamenchisaurid taxonomic revision is far beyond the scope of this paper. Reexamination of specimens referred to the type species (*M. constructus* and *O. junghsiensis*) would be a reasonable starting point, because the generic and specific diagnosis remains challenging with referred materials from different stratigraphic units (e.g., Young, 1958). Meanwhile, a temporary

solution may be to exercise caution in using the generic names for other referred species until the generic diagnosis is resolved. A thorough cladistic analysis of all mamenchisaurids should serve as a guideline for recombination and formulation of taxonomic names. This process is underway by the authors. In the presence of many species referred to the two genera, and in the absence of species-level phylogeny of mamenchisaurids, it may be desirable to establish a generic distinction for distinct mamenchisaurid taxa.

The holotype of *Qijianglong* likely represents an immature individual because the sutures between the braincase elements remain unfused in the holotype. In comparison with the holotype of *M. youngi*, the skull is approximately 25% larger, and the axis is comparable in length (approximately 10% longer in *Qijianglong*; Tables S1, S2; Ouyang and Ye, 2002). Each anterior cervical vertebra (3rd–6th) of *Qijianglong* has a centrum both absolutely and relatively longer than in *M. youngi* (Fig. 17). However, each of the mid-cervical vertebrae (7th–10th) has a both absolutely and relatively shorter centrum in *Qijianglong* than in *M. youngi*. The posterior cervical vertebrae (11th onward) of *Qijianglong* have comparable length/height ratio of the centra with *M. youngi*, but absolutely shorter and lower than those of *M. youngi*. Length/height ratios of the cervical vertebrae follow similar trends in mamenchisaurids. *M. hochuanensis* differs from smaller mamenchisaurids in that the centra of the anterior cervical vertebrae are not exceedingly more elongate than those of the cervical vertebrae that follow in the series (Fig. 17). Also in this taxon, the length/height ratios tend to be lower than in other mamenchisaurids. However, the absolute (numerical) length of the vertebral centra is greatest between the 9th and 13th cervical vertebrae in all mamenchisaurids examined, regardless of the relative length.

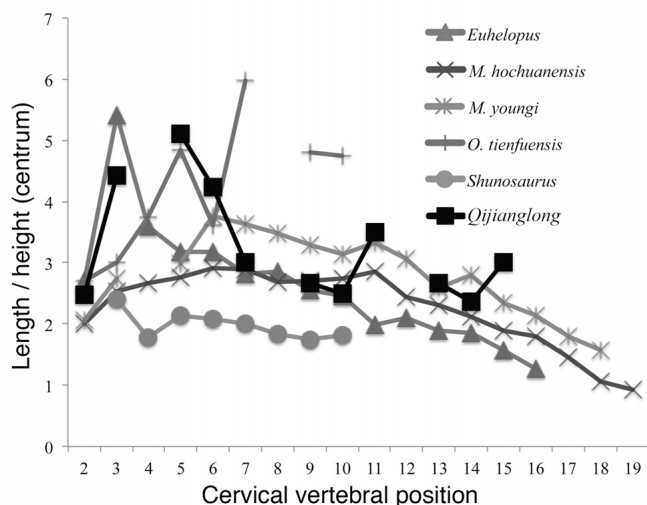


FIGURE 17. Comparison of length/height ratios of the cervical vertebral centra among representative sauropods from China with a relatively complete cervical series. *Euhelopus* is chronologically and systematically distant from *Qijianglong* but is included because it shows similar proportions of the cervical vertebral centra to those of *Qijianglong*. Measurements for the atlas are excluded. The lengths were taken as the maximum horizontal distance between the anterior and posterior articular surfaces, and the heights were taken as the vertical diameter of the posterior articular surface. The original measurements are available in Supplementary Data. Specimens from which measurements were taken: *Euhelopus zdanskyi* (PMU 233); *Mamenchisaurus hochuanensis* (holotype; Young and Zhao, 1972); *Mamenchisaurus youngi* (ZDM 83; Ouyang and Ye, 2002); *Omeisaurus tienfuensis* (ZDM T5703; He et al., 1988); *Qijianglong guokr* (QJGPM 1001); and *Shunosaurus* (ZDM T5401).

Some of these proportional differences may be taxonomically informative, but neither neck length nor individual vertebral length necessarily increases isometrically with respect to body size. It is possible that the cervical vertebrae have allometric growth in length within each species of mamenchisaurids (ontogenetic allometry) or among species (interspecific allometry). Although sample size is insufficient to test these hypotheses, the fact that the holotype of *M. youngi* has an absolutely longer neck than that of *Qijianglong* but a similar skull size suggests that proportional differences may be taxonomically meaningful at similar body sizes. However, the proportional differences should not be used in comparison with substantially larger or smaller specimens of mamenchisaurids until the ontogenetic and interspecific allometries of cervical vertebrae are well resolved among mamenchisaurids.

Despite the immature status of the holotype, *Qijianglong* is still distinguished from other mamenchisaurids and other sauropods by a number of autapomorphies. With the exception of one proportional character (semi-equal frontal and parietal lengths), all diagnostic characters are discrete (see Diagnosis). Although the discrete nature of the characters does not rule out the possibility of ontogenetic or allometric transformation, these diagnostic characters do not occur in *M. youngi*, which is of similar body size. Stratigraphically, both *Qijianglong* and *M. anyuensis* occur in the Suining Formation. Most notably among these differences, the cervical vertebrae of *M. anyuensis* are clearly distinguished from those of *Qijianglong* because they lack the finger-like process beside the postzygapophysis (He et al., 1996).

ACKNOWLEDGMENTS

The authors thank directors, collections managers, and curators at numerous institutions that they visited for this project. T. M. especially thanks those at the Institute of Vertebrate Paleontology and Paleoanthropology, Zigong Dinosaur Museum, and Qijiang Petrified Wood and Dinosaur Footprint National Geological Park Museum (China) for access to specimens in their care and for their hospitality. O. Mateus (Universidade Nova de Lisboa, Portugal), J. D. Harris (Dixie State College, U.S.A.), E. B. Koppelhus, K. Miyashita, and W. S. Persons (University of Alberta, Canada), P. Upchurch (University College London, U.K.), J. A. Wilson (University of Michigan, U.S.A.), and H.-L. You (Institute of Geology, China) provided discussion, data sets, and/or logistic support. A. Paulina Carabajal and O. Wings provided careful reviews, and P. Druckenmiller and H.-L. You's attention to detail improved the style and presentation of the manuscript. Financial aid for this project came from Qijiang County Bureau of Land and Resources, Chongqing, China (to L. X.), Vanier CGS and Alberta Innovates PGS (to T.M.), and NSERC (to P.J.C.). Author contributions: L.X., J.Z., D.L., and F.W. conducted the field work and did the initial research. T.M. and L.X. executed description and comparison. L.X., T.M., J.Z., D.L., Y.Y., T.S., F.W., and P.J.C. provided materials and analytical tools. T.M., L.X., and P.J.C. drafted the manuscript.

LITERATURE CITED

- Balanoff, A. M., G. S. Bever, and T. Ikejiri. 2010. The braincase of *Apatosaurus* (Dinosauria: Sauropoda) based on computed tomography of a new specimen with comments on variation and evolution in sauropod neuroanatomy. *American Museum Novitates* 3677:1–29.
- Barrett, P. M., and P. Upchurch. 2005. Sauropodomorph diversity through time: possible macroevolutionary and palaeoecological implications; pp. 125–156 in K. A. Curry-Rogers and J. A. Wilson (eds.), *Sauropod Evolution and Paleobiology*. University of California Press, Berkeley, California.
- Benton, M. J., L. Juul, G. W. Storrs, and P. M. Galton. 2000. Anatomy and systematics of the prosauropod *Thecodontosaurus antiquus* from the Upper Triassic of southwest England. *Journal of Vertebrate Paleontology* 20:77–108.

- Calvo, J. O., and L. Salgado. 1995. *Rebbachisaurus tessonei* sp. nov. A new Sauropoda from Albian-Cenomanian of Argentina; new evidence on the origin of the Diplodocidae. *Gaia* 11:13–33.
- Chatterjee, S., and Z. Zheng. 2002. Cranial anatomy of *Shunosaurus*, a basal sauropod dinosaur from the Middle Jurassic of China. *Zoological Journal of the Linnean Society* 136:145–169.
- Chatterjee, S., and Z. Zheng. 2004. Neuroanatomy and dentition of *Camarasaurus lentus*; pp. 199–211 in V. Tidwell and K. Carpenter (eds.), *Thunder-Lizards: The Sauropodomorph Dinosaurs*. Indiana University Press, Bloomington, Indiana.
- Curry Rogers, K., and C. A. Forster. 2004. The skull of *Rapetosaurus krausei* (Sauropoda: Titanosauria) from the Late Cretaceous of Madagascar. *Journal of Vertebrate Paleontology* 24:121–144.
- Díaz, V. D., X. P. Suberbiola, and J. L. Sanz. 2011. Braincase anatomy of titanosaurian sauropod *Lirainosaurus astibiae* from the Late Cretaceous of Iberian. *Acta Palaeontologica Polonica* 56:521–533.
- Dong, Z. M. 1997. A gigantic sauropod (*Hudiesaurus sinojapanorum*, gen. et sp. nov.) from the Turpan Basin, China; pp. 91–96 in Z.-M. Dong (ed.) *Sino-Japanese Silk Road Dinosaur Expedition*. China Ocean Press, Beijing, China. [Chinese, with English abstract]
- Galton, P. M. 1984. Cranial anatomy of the prosauropod dinosaur *Plateosaurus* from the Knollenmergel (Middle Keuper, Upper Triassic) of Germany. *Geologica et Palaeontologica* 18:139–171.
- Galton, P. M., and F. Knoll. 2006. A saurischian dinosaur braincase from the Middle Jurassic (Bathonian) near Oxford, England: from the theropod *Megalosaurus* or the sauropod *Cetiosaurus*? *Geological Magazine* 143:905–921.
- García, R. A., A. Paulina Carabajal, and L. Salgado. 2008. A new titanosaurian braincase from the Allen Formation (Campanian–Maastriachian), Río Negro Province, Patagonia, Argentina. *Geobios* 41:625–633.
- Gu, X., X. Liu, and Z.-F. Li. 1997. Stratigraphy of Sichuan Province. China University of Geosciences Press, Wuhan, China, 417 pp.
- Harris, J. D. 2006a. Cranial osteology of *Suuwassea emiliae* (Sauropoda: Diplodocoidea: Flagellicaudata) from the Upper Jurassic Morrison Formation of Montana, U.S.A. *Journal of Vertebrate Paleontology* 26:88–102.
- Harris, J. D. 2006b. The significance of *Suuwassea emiliae* (Dinosauria: Sauropoda) for flagellicaudatan interrelationships and evolution. *Journal of Systematic Palaeontology* 4:185–198.
- He, X.-L., C. Li, and K.-J. Cai. 1988. The Middle Jurassic Dinosaur Fauna from Dashampu, Zigong, Sichuan: Sauropod Dinosaurs. Volume 4, *Omeisaurus tianfuensis*. Sichuan Publishing House of Science and Technology, Chengdu, 143 pp. [Chinese, with English summary]
- He, X., S. Yang, K. Cai, K. Li, and Z. Liu. 1996. [A new species of sauropod, *Mamenchisaurus anyuensis* sp. nov.]; pp. 83–86 in *Papers on Geosciences Contributed to the 30th International Geological Congress*. Chengdu University of Technology, Chengdu, China. [Chinese]
- Hopson, J. A. 1979. Paleoneurology; pp. 39–146 in C. Gans, R. G. Northcutt, and P. Ulinski (eds.), *Biology of the Reptilia*, Volume 9. Academic Press, New York.
- Huene, F. von. 1932. Die Fossile Reptil-ordnung Saurischia: Ihre Entwicklung und Geschichte. Gebrüder Borntraeger. *Monographien Geologie und Paläontologie*, Series 1 4:1–361.
- Janensch, W. 1935. Die Schädel der Sauropoden *Brachiosaurus*, *Barosaurus* und *Dicraeosaurus* aus den Tendaguru-Schichten Deutsch-Ostafrikas. *Palaeontographica Supplement* to 7(1):147–298.
- Kan, Z.-Z., B. Liang, Q.-W. Wang, and B. Zhu. 2005. Trace fossils in the Suining and Penglaizhen Formations as buried places of dinosaur fossils, in Anyue, Sichuan, and their environmental significance. *Acta Geologica Sichuan* 25:68–71.
- Knoll, F., R. C. Ridgely, F. Ortega, J. L. Sanz, and L. M. Witmer. 2013. Neurocranial osteology and neuroanatomy of a Late Cretaceous titanosaurian sauropod from Spain (*Ampleosaurus* sp.). *PLoS ONE* 8:e54991. doi: 10.1371/journal.pone.0054991.
- Knoll, F., L. M. Witmer, F. Ortega, R. C. Ridgely, and D. Schwarz-Wings. 2012. The braincase of the basal sauropod dinosaur *Spinophorosaurus* and 3D reconstructions of the cranial endocast and inner ear. *PLoS ONE* 7:e30060. doi:10.1371/journal.pone.0030060
- Läng, E., and F. Mahammed, 2010. New anatomical data and phylogenetic relationship of *Chebsaurus algeriensis* (Dinosauria, Sauropoda) from the Middle Jurassic of Algeria. *Historical Biology* 22:142–164.
- Li, G., H. Hirano, T. Sakai, T. Kozai, and H. Ishiguro. 2010. Palaeontology and biostratigraphy of Jurassic clam shrimps of the Sichuan Basin, China. *Earth Science Frontiers* 17, special issue (Short Papers for the 8th International Congress on the Jurassic System):34–36.
- Li, K., C. Yang, J. Liu, and T. Jiang. 2010a. The vertebrate assemblages from the Shaximiao Formation of the Sichuan Basin, China and discussion to its age. *Earth Science Frontiers* 17, supplement (Short Papers for the 8th International Congress on the Jurassic System):123–124.
- Li, K., C.-Y. Yang, J. Liu, and Z.-X. Wang. 2010b. A new sauropod from the Lower Jurassic of Huili, Sichuan, China. *Vertebrata Palasiatica* 48:185–202.
- Lü, J., T. Li, S. Zhong, Q. Ji, and S. Li. 2008. A new mamenchisaurid dinosaur from the Middle Jurassic of Yuanmou, Yunnan Province, China. *Acta Geologica Sinica* 82:17–26.
- Lü, J., T. Li, Q. Ji, G. Wang, J. Zhang, and Z. Dong. 2006. New eusauro-pod dinosaur from Yuanmou of Yunnan Province. *Acta Geologica Sinica* 80:1–10.
- Lü, J., L. Xu, H. Pu, X. Zhang, S. Jia, H. Chang, J. Zhang, and X. Wei. 2013. A new sauropod dinosaur (Dinosauria, Sauropoda) from the late Early Cretaceous of the Ruyang Basin (central China). *Cretaceous Research* 44:202–213.
- Mannion, P. D., P. Upchurch, M. T. Carrano, and P. M. Barrett. 2011. Testing the effect of the rock record on diversity: a multidisciplinary approach to elucidating the generic richness of sauropodomorph dinosaurs through time. *Biological Reviews* 86:157–181.
- Marsh, O. C. 1878. Principal characters of American Jurassic dinosaurs (Part 1). *American Journal of Science*, Series 3 16:411–416.
- Monbaron, M., D. A. Russell, and P. Taquet. 1999. *Atlasaurus imerakei* n. g., n. sp., a brachiosaurid-like sauropod from the Middle Jurassic of Morocco. *Comptes Rendus de l'Académie des Sciences, Paris: Sciences de la Terre et des Planètes* 329:519–526.
- Nair, J. P., and S. W. Salisbury. 2012. New anatomical information on *Rhoetosaurus browni* Longman, 1926, a gravisaurian sauropodomorph dinosaur from the Middle Jurassic of Queensland, Australia. *Journal of Vertebrate Paleontology* 32:369–394.
- Ouyang, H., and Y. Ye. 2002. The First Mamenchisaurian Skeleton with Complete Skull: *Mamenchisaurus youngi*. Sichuan Science and Technology Press, Chengdu, China, 111 pp. [Chinese, with English summary]
- Paulina Carabajal, A. 2012. Neuroanatomy of titanosaurid dinosaurs from the Upper Cretaceous of Patagonia, with comments on endocranial variability within Sauropoda. *The Anatomical Record* 295:2141–2156.
- Paulina Carabajal, A., and L. Salgado. 2007. Un basicráneo de titanosaurio (Dinosauria, Sauropoda) del Cretácico Superior del norte de Patagonia: descripción y aportes al conocimiento del oído interno de los dinosaurios. *Ameghiniana* 44:109–120.
- Peng, G.-Z., Y. Ye, and Y. Gao. 2005. *Jurassic Dinosaur Faunas in Zigong*. People's Publishing House of Sichuan Province, Chengdu, China, 236 pp.
- Poropat, S. F., and B. P. Kear. 2013. Photographic atlas and three-dimensional reconstruction of the holotype skull of *Euhelopus zdanskyi* with description of additional cranial elements. *PLoS ONE* 8:e79932. DOI: 10.1371/journal.pone.0079932
- Remes, K. 2006. Revision of the Tendaguru sauropod dinosaur *Tornieria africana* (Fraas) and its relevance for sauropod paleobiogeography. *Journal of Vertebrate Paleontology* 26:651–669.
- Remes, K., F. Ortega, I. Fierro, U. Joger, R. Kosma, J. M. Marin Ferrer, Project Paldes, Project SNHM, O. A. Ide, and A. Maga. 2009. A new basal sauropod dinosaur from the Middle Jurassic of Niger and the early evolution of Sauropoda. *PLoS ONE* 4:e6924. doi: 10.1371/journal.pone.0006924.
- Royo-Torres, R., and P. Upchurch. 2012. The cranial anatomy of the sauropod *Turiasaurus riodevensis* and implications for its phylogenetic relationships. *Journal of Systematic Palaeontology* 10:553–583.
- Royo-Torres, R., A. Cobos, and L. Alcalá. 2006. A giant European dinosaur and a new sauropod clade. *Science* 314:1925–1927.
- Royo-Torres, R., A. Cobos, L. Luque, A. Aberasturi, E. Espílez, I. Fierro, A. González, L. Mampel, and L. Alcalá. 2009. High European sauropod dinosaur diversity during Jurassic-Cretaceous transition in Riodeva (Teruel, Spain). *Palaeontology* 52:1009–1027.
- Russell, D. A. 1993. The role of Central Asia in dinosaur biogeography. *Canadian Journal of Earth Sciences* 30:2002–2012.

- Russell, D. A., and Z. Zheng. 1993. A large mamenchisaurid from the Junggar Basin, Xinjiang, People Republic of China. *Canadian Journal of Earth Sciences* 30:2082–2095.
- Salgado, L., and J. Bonaparte. 1991. Un nuevo saurópodo Dicraeosauridae, *Amargasaurus cazau* gen. et sp. nov. de la Formación La Amarga, Neocomiano de la Provincia del Neuquén, Argentina. *Ameghiniana* 28:333–346.
- Sanz, J. L., J. E. Powell, J. Le Loeuff, R. Martínez, and X. Pereda-Suberbiola. 1999. Sauropod remains from the Upper Cretaceous of Laño (north central Spain). Titanosaur phylogenetic relationships. *Estudios del Museo de Ciencias Naturales de Alava* 14:235–255.
- Seeley, H. G. 1887. On the classification of the fossil animals commonly named Dinosauria. *Proceedings of the Royal Society of London* 43:165–171.
- Sekiya, T. 2011. Re-examination of *Chuanjiesaurus anaensis* (Dinosauria: Sauropoda) from the Middle Jurassic Chuanjie Formation, Lufeng County, Yunnan Province, southwest China. *Memoir of the Fukui Prefectural Dinosaur Museum* 10:1–54.
- Sereno, P. C., J. A. Wilson, L. M. Witmer, J. A. Whitlock, A. Maga, O. Ide, and T. A. Rowe. 2007. Structural extremes in a Cretaceous dinosaur. *PLoS ONE* 2:e1230. doi: 10.1371/journal.pone.0003303.
- Sereno, P. C., A. L. Beck, D. B. Duthiel, H. C. E. Larsson, G. H. Lyon, B. Moussa, R. W. Sadleir, C. A. Sidor, D. J. Varricchio, G. P. Wilson, and J. A. Wilson. 1999. Cretaceous sauropods from the Sahara and the uneven rate of skeletal evolution among dinosaurs. *Science* 286:1342–1347.
- Suteethorn, S., J. Le Loeuff, E. Buffetaut, V. Suteethorn, and K. Wongko. 2013. First evidence of a mamenchisaurid dinosaur from the Late Jurassic/Early Cretaceous Phu Kradung Formation of Thailand. *Acta Palaeontologica Polonica* 58:459–469.
- Swofford, D.L. 2003. PAUP*: Phylogenetic Analysis Using Parsimony, version 4.0b10. Sinauer Associates, Sunderland, Massachusetts.
- Tang, F., X. Jing, X. Kang, and G. Zhang. 2001. *Omeisaurus maoianus*: A Complete Sauropod from Jingyuan, Sichuan. China Ocean Press, Beijing, China, 128 pp. [Chinese, with English summary]
- Taylor, M. P. 2009. A re-evaluation of *Brachiosaurus altithorax* Riggs 1903 (Dinosauria, Sauropoda) and its generic separation from *Giraffatitan brancai* (Janensch 1914). *Journal of Vertebrate Paleontology* 29:787–806.
- Tidwell, V., and K. Carpenter. 2003. Braincase of an Early Cretaceous titanosauriform sauropod from Texas. *Journal of Vertebrate Paleontology* 23:176–180.
- Upchurch, P. 1995. The evolutionary history of sauropod dinosaurs. *Philosophical Transactions of the Royal Society of London, Series B* 349:365–390.
- Upchurch, P., and P. D. Mannion. 2009. The first diplodocid from Asia and its implications for the evolutionary history of sauropod dinosaurs. *Palaeontology* 52:1195–1207.
- Upchurch, P., P. M. Barrett, and P. Dodson. 2004. Sauropoda; pp. 259–322 in D. B. Weishampel, H. Osmólska, and P. Dodson (eds.), *The Dinosauria*, second edition. University of California Press, Berkeley, California.
- Wang, Y., B. Fu, X. Xie, G. Li, Q. Huang, X. Yang, Y. Pan, N. Tian, and Z. Jiang. 2010. The non-marine Triassic and Jurassic system in the Sichuan Basin, stratigraphic sequences, biodiversity and major strato-boundaries. *Earth Science Frontiers* 17, special issue (Short Papers for the 8th International Congress on the Jurassic System):19–21.
- Whitlock, J. A., M. D. D’Emic, and J. A. Wilson. 2011. Cretaceous diplodocids in Asia? Re-evaluating the phylogenetic affinities of a fragmentary specimen. *Palaeontology* 54:351–364.
- Wilson, J. A. 1999. A nomenclature for vertebral laminae in sauropods and other saurischian dinosaurs. *Journal of Vertebrate Paleontology* 19:639–653.
- Wilson, J. A. 2005. Redescription of the Mongolian sauropod *Nemegtosaurus mongoliensis* Nowinski (Dinosauria: Saurischia) and comments on Late Cretaceous sauropod diversity. *Journal of Systematic Palaeontology* 3:283–318.
- Wilson, J. A., and P. Upchurch. 2009. Redescription and reassessment of the phylogenetic affinities of *Euhelopus zdanskyi* (Dinosauria: Sauropoda) from the Early Cretaceous of China. *Journal of Systematic Palaeontology* 7:199–239.
- Wilson, J. A., M. S. Malkani, and P. D. Gingerich. 2005. A sauropod braincase from the Pab Formation (Upper Cretaceous, Maastrichtian) of Balochistan, Pakistan. *Gondwana Geological Magazine* 8:101–109.
- Wilson, J. A., M. D. D’Emic, T. Ikejiri, E. M. Moacdieh, and J. A. Whitlock. 2011. A nomenclature for vertebral fossae in sauropods and other saurischian dinosaurs. *PLoS ONE* 6:e17114. doi: 10.1371/journal.pone.0017114.
- Wings, O., D. Schwarz-Wings, and D.W. Fowler. 2011. New sauropod material from the Late Jurassic part of the Shishugou Formation (Junggar Basin, Xinjiang, NW China). *Neues Jahrbuch für Geologie und Paläontologie, Abhandlungen* 262:129–150.
- Wings, O., M. Rabi, J. Schneider, L. Schwermann, G. Sun, C.-F. Zhou, and W. Joyce. 2012. An enormous Jurassic turtle bone bed from the Turpan Basin of Xinjiang, China. *Naturwissenschaften* 99:925–935.
- Witmer, L. M., R. C. Ridgely, D. L. Dufeu, and M. C. Semones. 2008. Using CT to peer into the past: 3D visualization of the brain and ear regions of birds, crocodiles, and nonavian dinosaurs; pp. 67–87 in H. Endo and R. Frey (eds.), *Anatomical Imaging: Towards a New Morphology*. Springer, Tokyo.
- Wu, W.-H., C.-F. Zhou, O. Wings, T. Sekiya, and Z.-M. Dong. 2013. A new gigantic sauropod dinosaur from the Middle Jurassic of Shan-shan, Xinjiang. *Global Geology* 32:437–446.
- Xie, X., Y. Wang, and B. Fu. 2010. Sedimentary facies of the Upper Jurassic Suining and Penglaizhen formations in the central Sichuan Basin, SW China. *Earth Science Frontiers* 17, special issue (Short Papers for the 8th International Congress on the Jurassic System):313–314.
- Xing, L.-D., T. Miyashita, P. J. Currie, H.-L. You, and Z.-M. Dong. 2013. A new basal eusauropod from the Middle Jurassic of Yunnan Province, People’s Republic of China. *Acta Palaeontologica Polonica*. doi: 10.4202/app.2012.0151.
- Young, C.-C. 1958. New sauropods from China. *Vertebrata Palasiatica* 2:1–29.
- Young, C.-C., and X.-J. Zhao. 1972. *Mamenchisaurus hochuanensis*. Institute of Vertebrate Paleontology and Paleoanthropology Monograph Series I 8:1–30. [Chinese]
- Zhang, Y.-G., and J.-J. Li. 2003. Stratigraphy of the *Mamenchisaurus* fauna in Jingyan, Sichuan. *Journal of Stratigraphy* 27:50–53.

Submitted May 19, 2013; revisions received December 20, 2013; accepted January 25, 2014.

Handling editor: You Hailu.